NeuroImage 93 (2014) 276–291

Contents lists available at ScienceDirect

NeuroImage

journal homepage: www.elsevier.com/locate/ynimg

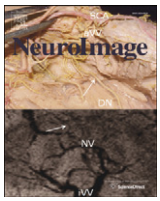

Review

An approach for parcellating human cortical areas using resting-state correlations

Gagan S. Wig [a,*,1], Timothy O. Laumann [a,1], Steven E. Petersen [a,b,c,d]

[a] Department of Neurology, Washington University School of Medicine, St. Louis, MO, USA
[b] Department of Psychology, Washington University School of Medicine, St. Louis, MO, USA
[c] Department of Radiology, Washington University School of Medicine, St. Louis, MO, USA
[d] Department of Anatomy and Neurobiology, Washington University School of Medicine, St. Louis, MO, USA

ARTICLE INFO

Article history:
Accepted 9 July 2013
Available online 19 July 2013

ABSTRACT

Resting State Functional Connectivity (RSFC) reveals properties related to the brain's underlying organization and function. Features related to RSFC signals, such as the locations where the patterns of RSFC exhibit abrupt transitions, can be used to identify putative boundaries between cortical areas (RSFC-Boundary Mapping). The locations of RSFC-based area boundaries are consistent across independent groups of subjects. RSFC-based parcellation converges with parcellation information from other modalities in many locations, including task-evoked activity and probabilistic estimates of cellular architecture, providing evidence for the ability of RSFC to parcellate brain structures into functionally meaningful units. We not only highlight a collection of these observations, but also point out several limitations and observations that mandate careful consideration in using and interpreting RSFC for the purposes of parcellating the brain's cortical and subcortical structures.

Contents

Introduction . . . 277
RSFC can be used to identify area borders in groups of individuals . . . 277
RSFC-Boundary Mapping identifies locations of abrupt transitions in patterns of resting-state correlations . . . 278
RSFC-defined borders are highly similar across independent groups of individuals . . . 278
RSFC-defined borders exhibit strong correspondence with task-activation maps . . . 279
Meta-analysis of task-evoked data reveals locations sensitive to a variety of signal types . . . 279
RSFC borders separate clusters of task-evoked data . . . 280
RSFC-defined borders respect architectonic divisions in some locations . . . 280
RSFC borders exhibit overlap with architectonic divisions defining primary visual cortex . . . 281
RSFC can be used to identify the locations of area centers . . . 282
RSFC-Snowball sampling identifies locations where resting-state correlation peaks aggregate . . . 283
RSFC-defined centers and borders compliment one-another . . . 283
RSFC-defined borders not only overlap with RSFC-defined system boundaries, but also reveal plausible areal divisions within the identified systems . . . 284
RSFC clusters, communities, and components are not equivalent to areas . . . 284
RSFC-defined area borders are consistent with RSFC-defined system boundaries in many locations . . . 284
RSFC-defined systems contain multiple areal divisions . . . 284
Additional constraints and considerations . . . 285
Relationship of RSFC-defined borders to BOLD signal strength . . . 285
Relationship of RSFC-defined borders to surface geometry . . . 286
RSFC-based parcellation of subcortical structures . . . 287
Concluding comments . . . 287
Acknowledgments . . . 287
Appendix A. Methods . . . 287
Subjects . . . 287

* Corresponding author at: Center for Vital Longevity, University of Texas at Dallas, 1600 Viceroy Drive, Suite 800, Dallas, TX, 75219, USA.
E-mail address: gwig@utdallas.edu (G.S. Wig).
[1] These authors contributed equally to this work.

1053-8119/$ – see front matter © 2013 Elsevier Inc. All rights reserved.
http://dx.doi.org/10.1016/j.neuroimage.2013.07.035

Data acquisition parameters . . . 287
Image preprocessing . . . 287
RSFC preprocessing . . . 288
Surface preprocessing . . . 288
RSFC-Boundary Mapping . . . 288
RSFC-Snowball sampling . . . 289
Conflict of interest . . . 290
References . . . 290

Introduction

The brain is organized at multiple spatial scales ranging from neurons to systems of functionally related areas (Sejnowski and Churchland, 1989). Area[2] parcellation has principally relied on discriminating areas based on the convergence of multiple underlying properties including function, architectonics (cyto-, mylo-, and chemo-), connectivity, and in some cases, topographic mapping (e.g., Felleman and Van Essen, 1991). An areal level of organization as revealed by distinctions in these properties is not limited to primary sensory areas (e.g., Foerster, 1936; Gennari, 1782; Hubel and Wiesel, 1962; Kaas et al., 1979; Marshall et al., 1937), but rather, is evident across the brain. For example, borders of area MT in the macaque monkey (also known as area V5) can be defined by MT's independent representation of the visual field, the presence of neurons with sensitivity to processing properties of visual motion, distinct patterns of incoming and outgoing connections, and the thick band of myelin that is present in layer IV (e.g., Van Essen et al., 1981). Likewise, distinctions in patterns of connectivity and architectonics have been used to parcellate ventral and medial frontal cortex into distinct areas in the macaque monkey (Carmichael and Price, 1994, 1996) and human (Ongur et al., 2003). While many of the tools used to identify areal boundaries have typically required invasive measurements or histological analysis of post-mortem brains, recent advances in brain imaging acquisition and analysis have offered an opportunity to parcellate brain areas non-invasively in living subjects (e.g., the present special issue on *In vivo Brodmann mapping in neuroimage*).

Defining areas using functional distinctions in humans has largely been accomplished by dissociating adjacent locations based on their patterns of task-evoked activity (e.g., Petersen et al., 1988; Sereno et al., 1995). More recently, attempts to functionally distinguish brain regions have leveraged the observation that the brain exhibits structured and ordered patterns of low-frequency functional correlations in the absence of overt task demands (Resting State Functional Connectivity (RSFC); Biswal et al., 1995). The prevalence of organized patterns of RSFC across levels of arousal makes RSFC well suited to understanding the function and organization of individuals that span ranges of age, mental health, and even species.

The precise significance of RSFC is uncertain; however, accumulating evidence suggests that resting-state correlations identify locations that are functionally similar with one another (for reviews see Biswal et al., 2010; Fox and Raichle, 2007). Furthermore, although RSFC relationships are likely mediated by anatomical connectivity, they are not restricted to direct structural connections (e.g., Honey et al., 2009; Vincent et al., 2007; for reviews see Deco et al., 2011; Wig et al., 2011). For these reasons, using resting-state correlations as a property by which to understand brain organization is likely drawing on information related to a combination of an area's functional role and its underlying anatomical connectivity.

RSFC has been used to identify putative areal divisions or boundaries by identifying locations where patterns of RSFC exhibit abrupt transitions (RSFC-Boundary Mapping; Cohen et al., 2008). RSFC-based area parcellations using boundary detection have been described for numerous locations including regions of the parietal cortex (Barnes et al., 2012; Nelson et al., 2010a), frontal cortex (Cohen et al., 2008; Hirose et al., 2012; Nelson et al., 2010b), and across expanses of the whole brain (Wig et al., 2013). Notably, there have been a number of additional applications of RSFC-based analysis with the goal of identifying areas (and also systems) in the brain (e.g., Deen et al., 2011; Doucet et al., 2011; Goulas et al., 2012; Kahnt et al., 2012; Kelly et al., 2010; Kim et al., 2010, 2013; Leech et al., 2012; Margulies et al., 2009; Mars et al., 2012; Mumford et al., 2010; Power et al., 2011; Ryali et al., 2013; Smith et al., 2009; Uddin et al., 2010; Yeo et al., 2011; Zhang et al., 2008). We return to the important distinction between boundary detection and alternate RSFC-based methods as means for area parcellation at a later point.

Rather than reviewing the growing body of work that has examined RSFC to identify brain areas and systems, we will utilize this article as a platform to describe some of our recent efforts towards parcellating large expanses of the cerebral cortex using patterns of RSFC. We recognize that the approaches for parcellating brain areas using patterns of RSFC are under continuous revision and refinement, and will continue to improve. Here we will highlight our groups most recent progress in this endeavor and provide descriptions of some important observations, caveats, and places for potential improvement in using RSFC to parcellate brain areas. Our aims are three-fold. First, we aim to demonstrate that the borders revealed by RSFC-Boundary Mapping reflect locations of RSFC pattern transition and are highly similar across independent groups of subjects. Second, we compare the results of RSFC-Boundary Mapping to areal distinctions revealed by other modalities (specifically, task-evoked activity and architectonics) to demonstrate the strong convergence across methods of parcellation in certain locations. Third, we contrast RSFC-Boundary Mapping to other RSFC-based methods that have been used to identify functional area centers or cluster groups of functionally related voxels across large expanses of the brain. Throughout the report, we will also draw attention to a number of observations and limitations for using RSFC to parcellate areas, and discuss their implications towards both the theory and practice of RSFC-based parcellation.

RSFC can be used to identify area borders in groups of individuals

Brain imaging permits areal parcellation in individual subjects and a related article describes our recent efforts towards this endeavor using RSFC (Wig et al., 2013). We draw attention to two observations from that report: (1) RSFC parcellation maps exhibit significantly higher similarity between independent scans of the same individual from different days than between scans from different individuals (see Wig et al., 2013, Fig. 11 and Supplementary Fig. 4). The between subject variability in RSFC parcellation is consistent with reports that have demonstrated subject-wise variability in brain area organization as defined by task-evoked activity (e.g., Dougherty et al., 2003; Fedorenko et al., 2010; Sabuncu et al., 2010), architectonics (e.g., Amunts et al., 2004; Caspers et al., 2006), anatomical connectivity (e.g., Johansen-Berg et al., 2005), and macroscopic anatomy (e.g., Van Essen, 2005). (2) Despite the presence of individual differences in area parcellation, numerous features revealed by RSFC parcellation are consistent across individuals (see Wig et al., 2013, Fig. 12). Accordingly, for the present work, rather

[2] The term 'area' is conventionally restricted to parcellations of the cerebral cortex and the discussion that follows largely focuses on cortical divisions. It should be noted however, that many of the general ideas regarding parcellation that will be discussed here are applicable to cortical areas as well as subdivisions of subcortical nuclei and the cerebellum.

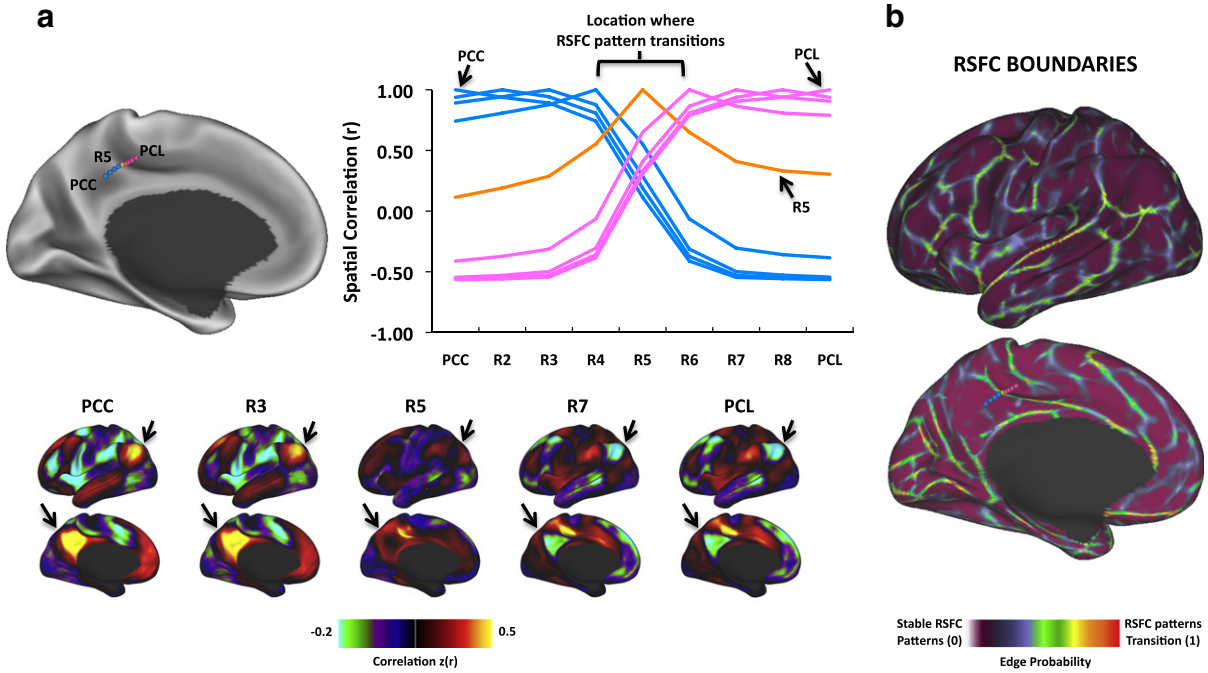

Fig. 1. Patterns of RSFC exhibit abrupt changes across the cortical surface. (a) RSFC maps were derived for locations (R2–R8) between a region in the posterior extent of the cingulate cortex (PCC) and a region in the paracentral lobe (PCL) in a group of subjects (n = 40; defined anatomically; locations are shown as colored balls). The plot to the right depicts the similarity (spatial correlation) of every location's RSFC map with the RSFC map of each of the other locations. RSFC maps are similar from PCC to R4, followed by a location of abrupt change (R5), and then a second set of locations where the maps are highly self-similar. Similarity lines and location balls have been color coded to denote greater RSFC similarity with PCC (blue) or PCL (pink). The location whose RSFC map was not similar to either the PCC or PCL group (R5) is color-coded orange. The RSFC maps of a subset of the regions are depicted on the lower panel, and two locations with prominent differences between maps are highlighted by arrows (the angular gyrus on the lateral views and anterior cingulate gyrus on the medial views). (b) RSFC-Boundary map for a group of subjects (n = 40). The coloring highlights where patterns of RSFC exhibit abrupt transitions (i.e., putative areal borders) and locations where patterns of RSFC are relatively stable. Locations highlighted in panel (a) are displayed on the medial surface — the identified transition point (orange) is at a location of high border likelihood.

than focusing on parcellating individual brains that exhibit numerous sources of variation, we adopt a strategy that highlights the commonalities across individuals from a single cohort and report 'group-based' parcellations. While a group-based strategy might obscure important and interesting parcellation variation within a population, it permits identification of the consistent parcellation features across the population.

There are a number of ways to derive a group-based RSFC parcellation. The primary difference across methods relates to the processing stage at which individuals are combined to create group estimates, and each alternative will potentially introduce the influence of different sources of variation. We refer the interested reader to Appendix A of this report for details of the methods we have used here to arrive at group-based RSFC parcellations.

RSFC-Boundary Mapping identifies locations of abrupt transitions in patterns of resting-state correlations

RSFC-Boundary Mapping rests on the assumption that an area's RSFC correlations are relatively uniform within the extent of an area, yet may be distinct from the RSFC of an adjacent area (Cohen et al., 2008). In this view, locations where the patterns of RSFC exhibit abrupt transitions can be considered putative boundaries between areas across the cortical surface. This concept is illustrated in Fig. 1. By computing and comparing the average seed-based RSFC maps from a group of young adults (N = 40) for a line of seeds across a portion of the cortical surface, we can see that the RSFC correlation maps do not change smoothly, but rather, exhibit rapid and abrupt changes (Fig. 1a). Furthermore, these locations of change are consistent in both directions (i.e., from an inferior location in the posterior extent of the cingulate gyrus to a more superior location in the paracentral lobe, or in reverse), suggesting the presence of a functional boundary between two adjacent areas. This basic approach can be extended across the cortical surface with the aid of image-processing tools to create a vertex-wise estimate of the likelihood with which a location is identified as an RSFC boundary (i.e., a spatial gradient of changes in correlation map similarity, or its corresponding edge [3]) between two locations in the brain (Fig. 1b; see Appendix A — Methods for method details). The RSFC boundary map reveals locations where patterns of RSFC exhibit a transition (hotter colors), and locations where the patterns of RSFC are more locally stable (cooler colors). We hypothesize that the locations of transitions are strong candidates for the locations of boundaries between distinct areas.

RSFC-defined borders are highly similar across independent groups of individuals

We argue that group-based parcellation may deemphasize some of the inherent variability across groups of individuals (both anatomical and otherwise) to reveal the parcellation features (in the current case, areal boundaries[4]) that are consistent across individuals. If this is the case, then RSFC-Boundary Mapping parcellations from independent groups of individuals sampled from the same cohort should be highly similar. Fig. 2a depicts the group-based RSFC Boundary Mapping maps

[3] Spatial gradient maps can exhibit features reflecting a high level of variability in the magnitude of correlation map changes (cf. Fig. 9 — step 6, and Wig et al., 2013), suggesting that even adjacent cortical areas identified in this way will not be equally separable from one another in terms of their patterns of RSFC. In the present work, we have applied an edge detection technique that emphasizes the locations where there is a gradient present. The edges are agnostic as to how large the correlation pattern change underlying the transition is. Thus large and small correlation pattern changes can both have high values in the edge probability map as long as the location of transition is consistently identified.

[4] Parcellation features may also include an area interior/extent or an area geometric center.

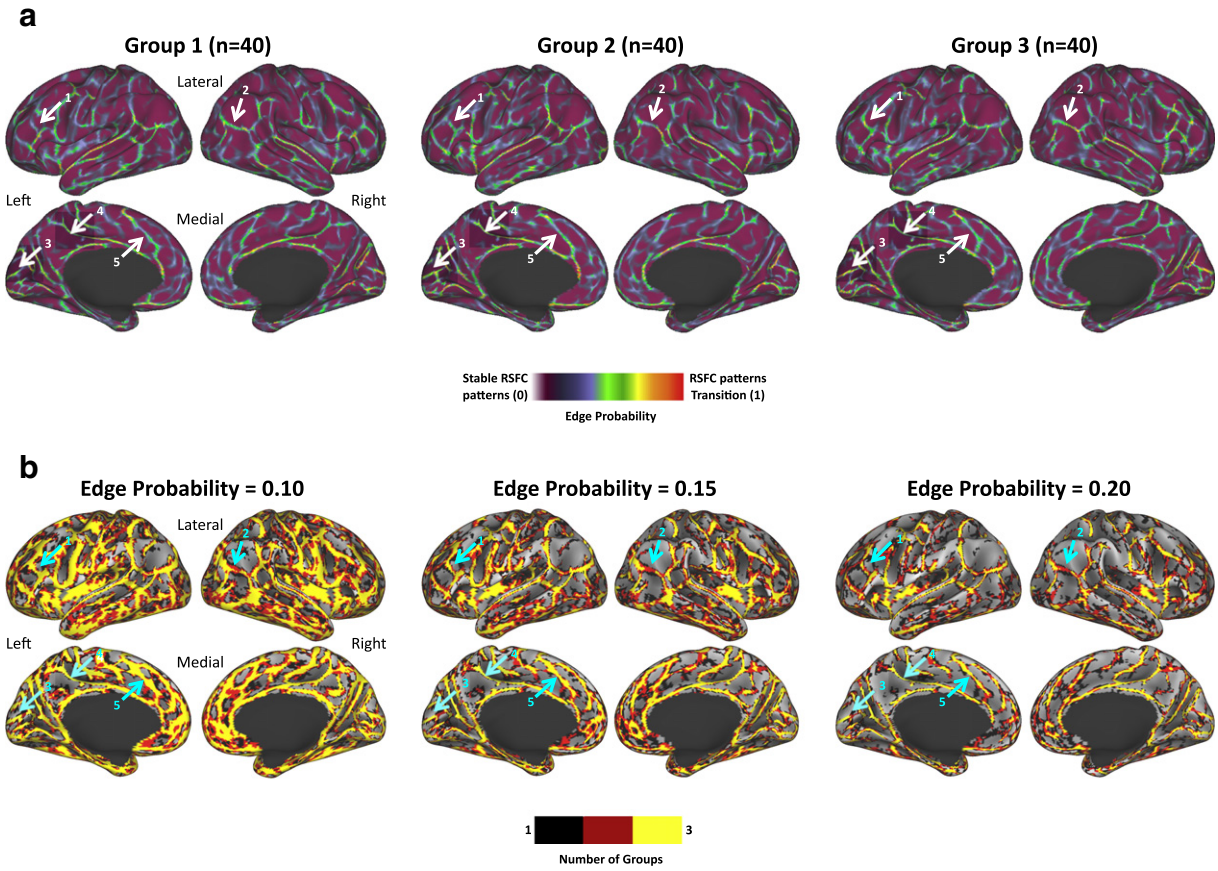

Fig. 2. RSFC-Boundary Mapping parcellation reliably identifies locations of putative area borders. (a) RSFC-Boundary Mapping parcellations are highly similar across 3 independent groups of healthy young adults. A subset of locations is pointed out with arrows to highlight the high degree of similarity in parcellations. These locations include regions along the inferior and middle frontal gyri of the left hemisphere (1), a strong border separating angular gyrus from the middle-occipital gyrus in the right hemisphere (2), a strong border parallel to the calcarine sulcus in the medial occipital lobe (3), a strong border separating posterior extent of the cingulate gyrus from locations in the paracentral lobe (4), and a border which separates locations in the anterior cingulate gyrus from more dorsal regions of the medial frontal cortex (5). (b) The strongest RSFC-Boundary Mapping borders are consistent across groups. Independent conjunction images created by first thresholding each of the three group's RSFC-Boundary Mapping parcellation maps from (a), binarizing the image, and summing the three images to demonstrate the consistency in parcellation features across groups. Three edge probability thresholds are depicted.

from three independent groups of healthy young adults (N = 40 individuals/group). The spatial correlation between the three parcellation maps reveals a high degree of similarity across the groups (average spatial correlation: r = 0.60, range of spatial correlations across three maps: r = 0.60–0.61). Visual inspection confirms that the locations of many of the putative boundaries between areas are strikingly similar across the three groups. For example, locations along the middle and inferior frontal gyri exhibit similar areal boundaries in each of the three groups providing evidence for distinct divisions along the lateral frontal cortex. Likewise, prominent boundaries within medial–superior frontal cortex, medial parietal cortex (e.g., between posterior cingulate cortex and paracentral lobule), medial occipital cortex, and lateral parietal cortex (e.g., between the angular gyrus and the lateral aspect of the middle occipital gyrus) are evident in all three groups. To demonstrate the overlap in group-based parcellations, each of the group maps was thresholded to reveal the strongest edge probability locations, and a conjunction of these images was created (Fig. 2b). Conjunction maps were created over a range of edge probability thresholds (0.10–0.20) to give a more complete picture of the amount of overlap in RSFC-Boundary Mapping features. The putative boundaries highlighted earlier can all be observed in these conjunction images, reinforcing their consistency. In addition, a final group-based parcellation was derived by combining the individuals from the three independent groups into one 120-subject group (Fig. 3). Not surprisingly, this last group parcellation map is similar to each of the independent group parcellations. This 120-subject group parcellation map includes the consistent features highlighted in the conjunction maps of Fig. 2b while also retaining the full range of edge probability values across all cortical vertices; it is used in our subsequent comparisons.

RSFC-defined borders exhibit strong correspondence with task-activation maps

To understand the relevance of RSFC-based areal boundaries, it is critical to determine whether parcellations derived from the current approach correspond with parcellations identified by other modalities. Brain areas perform distinct processing operations and an RSFC parcellation map should reveal areal divisions that are functionally plausible based on known processing dissociations. Previous research in both our laboratory and others has taken this approach to begin to inform and validate RSFC parcellations in numerous cortical locations (e.g., Nelson et al., 2010a; Wig et al., 2013, also see Smith et al., 2009). By examining functional activity defined by the meta-analysis of large batteries of task-evoked data, we identified a collection of independent locations demonstrating unique fingerprints of functional activity that converge with divisions revealed by RSFC borders.

Meta-analysis of task-evoked data reveals locations sensitive to a variety of signal types

Meta-analyses were conducted on a large collection of independent studies in which independent groups of subjects performed different

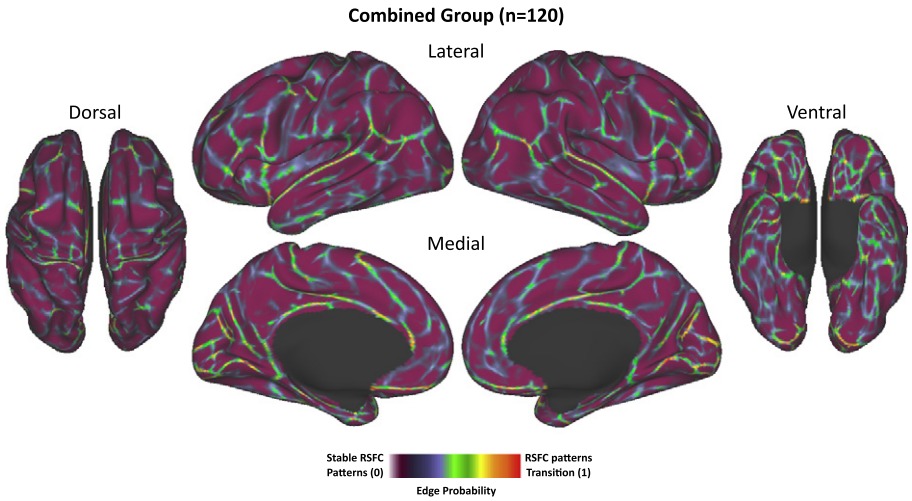

Fig. 3. RSFC-Boundary Mapping parcellation from combined group (N = 120) of healthy young adult subjects. The coloring highlights where patterns of RSFC exhibit abrupt transitions (i.e., putative areal borders) and locations where patterns of RSFC are relatively stable.

tasks with different stimuli. Each meta-analysis was aimed at identifying brain regions that reliably displayed significant activity when certain tasks were performed (e.g., reading) or certain signal types were expected (e.g., error-related activity). While the analyses were constrained by the available datasets (specifically those collected in our laboratory), we were able to create meta-analytic maps for task-evoked activity focused on error-related processing, task-induced deactivations, task-initiation, memory (episodic retrieval), language (reading), and sensorimotor functions. All study datasets contributing to the meta-analyses were acquired on a single scanner (a Siemens 1.5 Tesla Magnetom Vision MRI scanner), which was distinct from the scanner used to acquire the RSFC data (see Appendix A — Methods for details). For each dataset, the voxels passing a statistical threshold were identified to create a binary mask, and the resultant maps were summed to create a conjunction image for the corresponding meta-analysis (for subject, dataset and analysis details see Power et al., 2011). This conjunction image indicated how often a voxel was identified across all the datasets associated with the given task or signal-type. In this way, each meta-analytic conjunction image represents an estimate of the spatial extent of functional areas defined by task-related activity.

RSFC borders separate clusters of task-evoked data

For comparison to the RSFC-Boundary map, we focus on voxels exhibiting significant activity in at least 60% of the studies contributing to each task-evoked meta-analysis. As the comparison is constrained by available datasets, only a portion of the total cortical surface is available for comparison between modalities. Fig. 4 demonstrates that locations demonstrating task-induced activity tend to fall within borders defined by RSFC (for purposes of comparison, the 120-subject RSFC-Boundary map was thresholded at >0.15 edge probability to identify stronger borders). In several locations, RSFC-defined borders tightly surround clusters identified in task-evoked maps. For example, locations demonstrating task-induced deactivations including the medial prefrontal cortex, angular gyrus, and posterior cingulate cortex are surrounded by RSFC borders. In other locations, contiguous voxels of activity which appear to have multiple local maxima and associated sub-clusters are separated by an RSFC border, suggesting the sub-clusters may be parts of different areas (e.g., in the motor-response meta-analytic map a task-related cluster in the anterior portion of the cingulate gyrus is separated by an RSFC-border from a more dorsal cluster in the medial superior frontal cortex likely corresponding to the supplementary motor area, while in the episodic-memory meta-analytic map a task-related cluster in the inferior parietal lobule is separated by an RSFC-border from a cluster in the angular gyrus). As a quantitative confirmation of these qualitative observations, we performed a chi-square test of independence between a composite task-map of all cortical locations exhibiting task-evoked activity in at least one meta-analytic map and the thresholded RSFC-Boundary map. The vertices identified as having a high likelihood of being an RSFC-defined border and the vertices identified as exhibiting task-evoked data (i.e., putative area interiors) came from non-overlapping populations ($X2\,(1, N = 59{,}412) = 220.9, p \ll 0.001$).

It is important to note, however, that the correspondence between task-evoked activity and RSFC-borders is not perfect at all locations (e.g., not all task clusters are perfectly enclosed by RSFC borders). This may be a consequence of the large differences in data acquisition and processing between the two types of data (e.g., different scanners, volume-based analysis for task data vs. surface-based RSFC parcellation). Indeed, a thorough demonstration of the correspondence between RSFC-borders and task activations will require datasets that include both data types in the same subjects. This caveat notwithstanding, there may remain true discrepancies between these modalities that will mandate closer examination of the sources of disparity. Resting state and task-evoked activity may highlight different aspects of the brain's functional organization.

RSFC-defined borders respect architectonic divisions in some locations

In addition to functional dissociations, identifying the transitions in architectonic features has been a standard approach towards parcellating human cortical areas since (Brodmann, 1909). More recently, probabilistic maps of a collection of cortical areas have been defined by quantitative procedures that measure changes in the laminar distribution of cell-body density across the cortical surface in a set of post-mortem human brains (Amunts et al., 2000; Schleicher and Zilles, 1990; Schormann and Zilles, 1998). Surface-based representations of these maps, as well as a number of other parcellations, are available in the sumsDB database (http://sumsdb.wustl.edu/) and have been described at greater length elsewhere (Fischl et al., 2008; Van Essen et al., 2012). Direct comparisons between maps derived from post-mortem dissection of human brains and the in-vivo RSFC parcellation described hitherto have clear caveats towards interpretation. Determining the precise convergence between architectonics and RSFC will be best accomplished by incorporating imaging methods that can reveal cellular and sub-cellular features of anatomy, and there are numerous efforts to do so (Dick et al., 2012; Glasser and Van Essen, 2011; Toga et al., 2006). Keeping

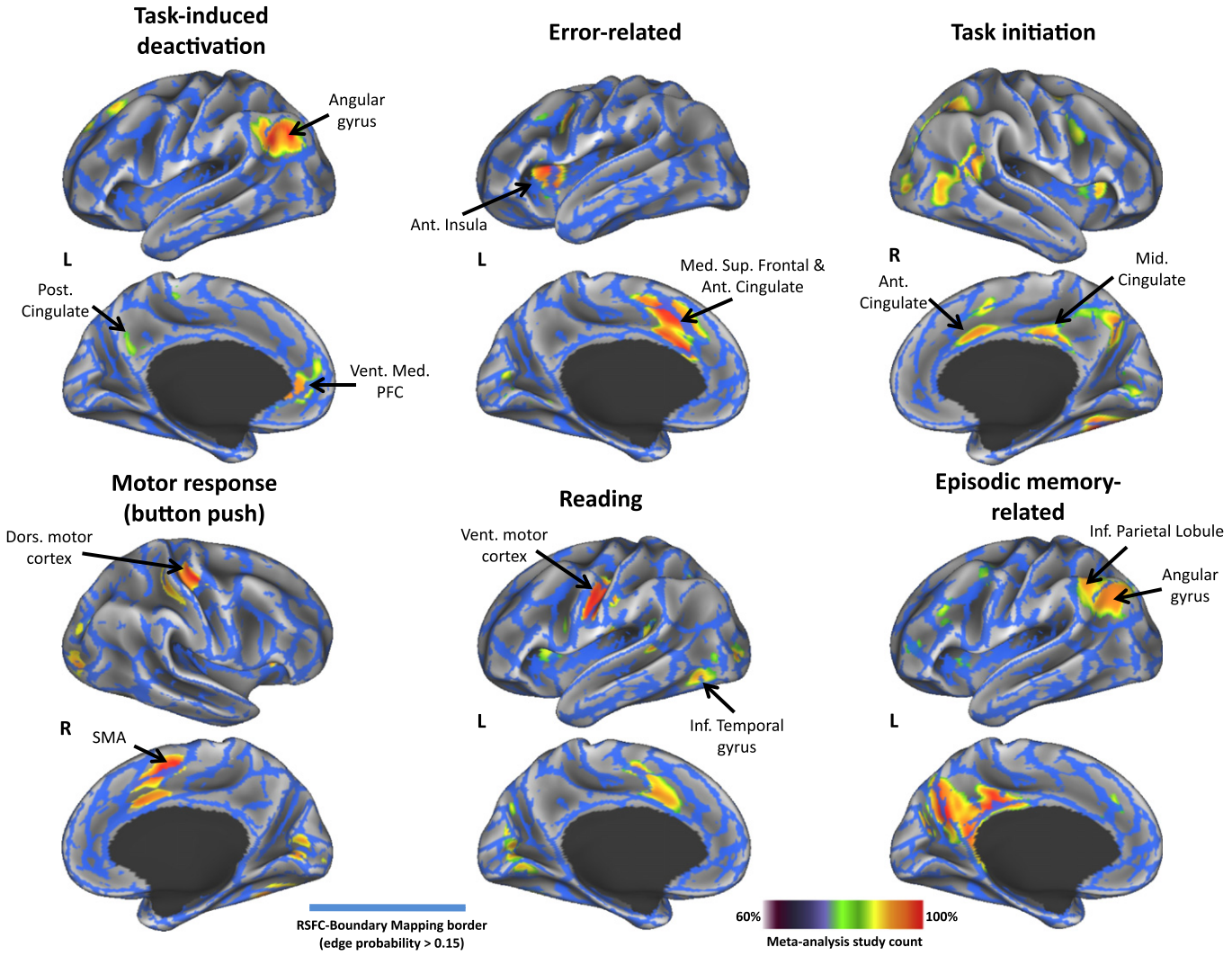

Fig. 4. RSFC-Boundary Mapping parcellation exhibits a high degree of correspondence with areas defined by task-evoked activity. Task-evoked activity was derived from meta-analyses of multiple studies to highlight locations exhibiting sensitivity to performance of certain tasks (e.g., reading) or certain signal types (e.g., error-related activity). The 120-subject RSFC-Boundary Mapping parcellation was thresholded (edge probability > 0.15) to reveal locations exhibiting a high likelihood of being a border between areas. Many area locations defined by task-evoked activity are surrounded by RSFC-borders (e.g., the cluster of activity in the ventral medial prefrontal cortex in the task-induced deactivation meta-analytic map). In other locations RSFC-borders separate what appear to be distinct clusters of task-evoked activity, suggesting the existence of distinct areas (e.g., a cluster of activity in the inferior parietal lobule is separated from a cluster of activity in the angular gyrus in the episodic memory meta-analysis map). Parcellations are overlaid on inflated cortical surfaces; some surfaces have been tilted to facilitate viewing (i.e., the lateral surface of the right hemisphere in the motor response (button pushing) comparison and the lateral surface of the left hemisphere in the error-related activity comparison).

this limitation in mind, we describe preliminary observations that suggest RSFC-based parcellations may converge with features related to underlying cellular anatomy.

RSFC borders exhibit overlap with architectonic divisions defining primary visual cortex

While the precise correspondence between probabilistic maps of cyto-architecture based on post-mortem histology and RSFC-based boundaries may be difficult to ascertain due to the very different methods and underlying properties used to create these parcellations, we highlight here an important instance where they appear to converge. Fig. 5a depicts the probabilistic estimates of areas 17 and 18 (herein referred to as probabilistic area (PA) 17 and 18). These architectonic areas have been shown to have reasonable correspondence with retinotopic maps of V1 and V2 (V1 more clearly than V2; Hinds et al., 2009; Van Essen et al., 2012). The architectonic boundaries are overlaid on a medial occipital view of the RSFC-Boundary map as black lines. The border between PA 17 and PA 18 overlaps with a prominent border in this map that runs both ventral and dorsal to the calcarine sulcus. These RSFC-based borders were also consistently observed in each of the individual group parcellations (see arrow '3' in Fig. 2).

Fig. 5b demonstrates how RSFC seed maps differ on either side of the RSFC-Boundary Mapping defined border (calculated across all 120 subjects). When a seed is placed ventral to the calcarine sulcus but dorsal to an RSFC-defined border (gray ball labeled '17' in Fig. 5a), resting-state correlations are prominent within PA 17 but bound by the RSFC-defined borders separating PA 17 from PA 18. Conversely, a seed region on the opposing side of the RSFC-defined border (gray ball labeled '18' in Fig. 5a) exhibits the strongest resting-state correlations with locations within PA 18, both dorsal and ventral to the calcarine sulcus. The difference between these two seed-based maps is best appreciated in the statistical difference image ($t(119) = 3.38$, $p < 0.001$); a collection of other more distal locations also exhibit differential connectivity as a function of seed location. Accordingly, the presence of a RSFC-defined border separating PA 17 from PA 18 likely reflects differences in both local and global correlation patterns.

Notably, there are additional borders found by RSFC-Boundary Mapping within PA 17. For example, a border running along the calcarine sulcus (red arrow, labeled '1') approximates the position of the

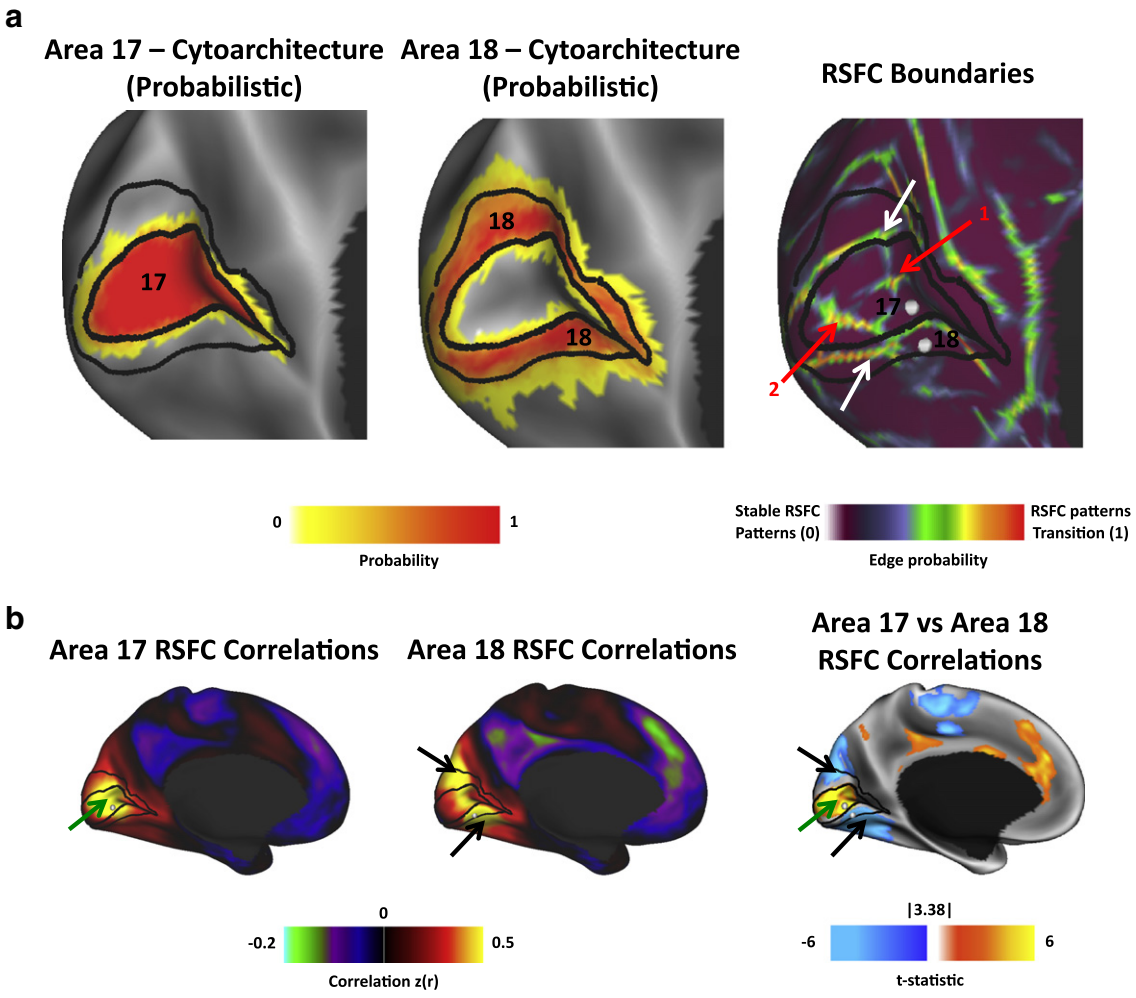

Fig. 5. RSFC-Boundary Mapping compared to cyto-architectonically-defined probabilistic areas (PA) 17 and 18. (a) Medial occipital view of PA 17 and PA 18 (Fischl et al., 2008) and 120-subject RSFC-Boundary map. Black lines indicate reasonable boundaries between and around areas 17 and 18 as described in Van Essen et al. (2012). The white arrows indicate dorsal and ventral RSFC boundaries that appear to closely correspond to the architectonic boundary. The RSFC-based borders are also apparent in each of the individual groups (see Fig. 2). Red arrow 1 indicates a boundary along the calcarine fissure that may correspond to the horizontal meridian of PA 17 (Visual Area 1). Red arrow 2 indicates a boundary that is likely due to susceptibility artifact at the occipital pole (see Fig. 8a). (b) Correlation maps generated from ventral PA 17 and PA 18 seeds (gray balls) and the differences between them. Green and black arrows highlight the locations of strongest correlations for seeds in PA 17 and PA 18, respectively. The differences between the two seeds can be best appreciated on the statistical difference map, which is calculated as a surface vertex-wise two-sample t-test between the correlation maps of the two seeds. Note that the contour of the difference image follows the PA 17/18 boundary.

horizontal meridian in retinotopic maps of V1 and may reflect differences in RSFC between the upper and lower visual fields of V1. Likewise a border running along the dorsal–ventral axis mid-way through PA 17 may divide the more central vs. peripheral visual representations of this area. The presence of additional borders within a cortical area characterized by topographic mapping is consistent with the RSFC-based division between mouth and hand regions of primary motor and somatosensory cortex that has been reported by network estimation methods elsewhere (e.g., Power et al., 2011; Yeo et al., 2011). This division of motor/somatosensory cortex can also be seen in the parcellation maps presented here (e.g., see borders surrounding the dorsal motor cortex surrounding button-push related task activity and in the ventral motor cortex surrounding reading-related task activity in Fig. 5). Importantly, a number of divisions are also apparent along the pre- and post-central gyri, and exhibit correspondence with other probabilistic area divisions (e.g., PA 1 vs. 2, PA 2 vs. 3b; see post-central gyrus in lateral views in Fig. 4). All together, these observations are critical to evaluate: they likely reflect the special nature of the information RSFC brings to bear towards understanding area organization and function but also stress caution when interpreting the presence of RSFC boundaries in the absence of parcellation information from other modalities.

The RSFC-Boundary Mapping border corresponding to the PA 17/PA 18 border extends somewhat further laterally beyond the occipital pole than the cyto-architectonic boundary (while a lateral view is not presented in Fig. 5, a lateral view of the RSFC-Boundary Mapping borders are presented in Fig. 3). This discrepancy, along with an aberrant border within PA 17 (Fig. 5a: red arrow, labeled '2'), may be due to inadequacies in the scan acquisition and processing — in particular, field distortions and/or signal loss related to vasculature at the occipital pole likely affected the position of borders measured here (see subsequent Additional constraints and considerations section and red arrow labeled '4' in Fig. 8a).

RSFC can be used to identify the locations of area centers

RSFC patterns can also be leveraged to reveal alternative features that may relate to area organization. So far, we have described how identifying locations where patterns of RSFC exhibit an abrupt transition can be used for identifying borders between putative areas. An alternative strategy is to focus on identifying the interior (or central) parts of areas rather than the boundaries between them. We use an RSFC approach that aims to directly identify these interior regions and suggests that RSFC-based areal center

identification may help parcellate areas that are not clearly distinguished by RSFC-Boundary Mapping (Wig et al., 2013). In general, these two approaches to RSFC-based area definition should be highly complimentary to one another.

RSFC-Snowball sampling identifies locations where resting-state correlation peaks aggregate

Our method for identifying candidate locations for the central portions of areas combines seed-based RSFC with principles inspired by social network science and graph theory (Snowball sampling; Goodman, 1961; Wasserman and Faust, 1994). RSFC-Snowball sampling first identifies the peaks of correlation (i.e., neighbors) from a seed-based RSFC map, and then iteratively tracks the neighbors of these neighbors through multiple stages. To minimize sampling bias, this basic process is repeated from numerous starting locations across the brain, and the output of each sampling procedure is aggregated to arrive at a final peak density map. We have previously described the details of using this method for parcellating an individual subject's cortical and subcortical brain structures; RSFC-Snowballing parcellation maps are reliable within an individual scanned over multiple days, and area center locations defined by RSFC-Snowballing correspond with area center locations defined by task-evoked data (Wig et al., 2013). To parallel the present group-based RSFC-Boundary Mapping parcellation observations, a method for extending the RSFC-Snowballing method to the level of groups is presented in the Appendix A section.

RSFC-defined centers and borders compliment one-another

An RSFC-Snowballing peak density map was derived for the group of 120 individuals. Rather than being randomly or uniformly distributed, the RSFC-Snowballing map exhibits a structured distribution, with some locations having many peaks, and others having very few. If RSFC-Boundary Mapping identifies the locations of putative boundaries between areas and RSFC-Snowballing identifies the locations of putative centers of areas, peak density values should be less prominent at locations that are transition points (or boundaries) and more prominent within boundary interiors. Simultaneously viewing the strong borders defined by RSFC-Boundary Mapping and the strong centers defined by RSFC-Snowballing suggests this expectation may be true (Fig. 6). Importantly, each of the two methods appears to reveal unique parcellation features in some locations (e.g., two area centers identified by RSFC-Snowballing in the posterior–inferior temporal cortex are surrounded by an area border defined by RSFC-Boundary Mapping on the lateral right hemisphere), suggesting the two methods are not completely redundant with one another and can be used in combination for the purposes of RSFC parcellation (for more detailed examples and discussion see Wig et al., 2013). This is consistent with the negative, but non-perfect relationship between the two RSFC-based parcellation maps ($r = -0.14$, $p << 0.001$).

The non-perfect relationship noted above may be surprising, given that both methods of area parcellation focus on patterns of RSFC. This observation may related to a practical as opposed to conceptual difference between the methods — operationally, the thresholds that are most useful for a given method of parcellation may miss distinctions in another method of parcellation and the different processing steps for each method may accentuate and attenuate non-overlapping sources of noise in RSFC. For example, adjacent areas that share very similar patterns of RSFC would have a weak boundary between them, yet the area centers might be highlighted by RSFC-Snowballing. Along these lines, there are trade-offs between methods that focus on borders between areas versus methods that attempt to identify area interiors. Relying on borders may result in parcellations with discontinuous boundaries if there are differences in the strength of RSFC transitions between an area and the various areas that are adjacent to it. Likewise, focusing on area centers may result in a parcellation with a poor

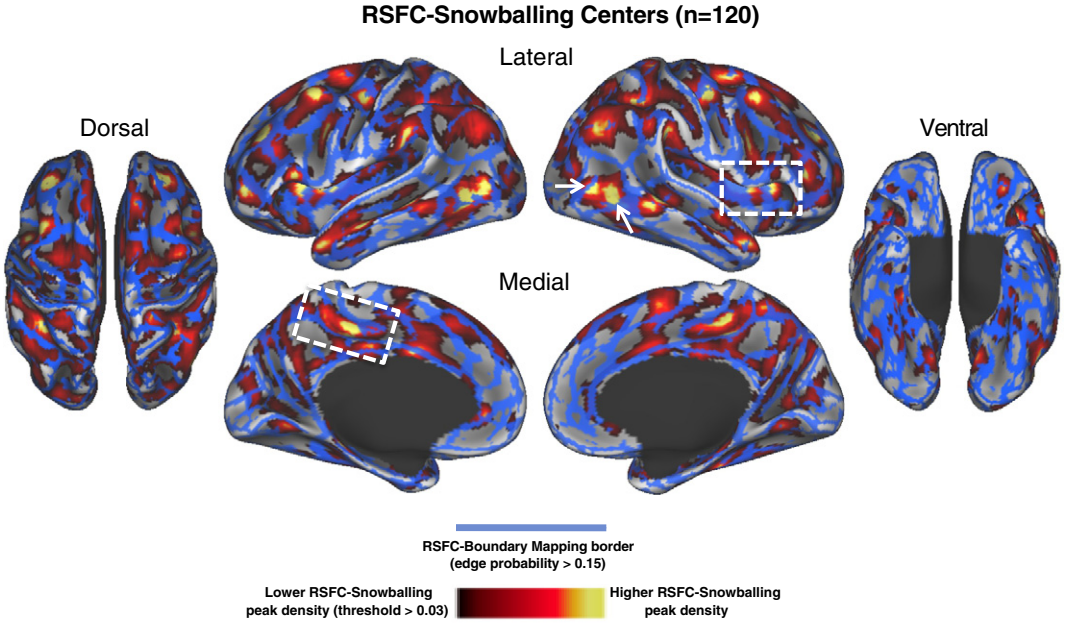

Fig. 6. Area borders defined by RSFC-Boundary Mapping surround area centers defined by RSFC-Snowballing. RSFC-Snowballing parcellation of 120 subjects reveals the locations of putative area interiors (centers). This RSFC-Snowballing parcellation map was thresholded to highlight vertices with high area center likelihood (peak density > 0.03). The 120-subject RSFC-Boundary Mapping parcellation was thresholded to reveal locations exhibiting a high likelihood (edge probability > 0.15) of being a border between areas. Each parcellation method reveals different area features (i.e., interiors and borders) and many locations exhibit a high degree of correspondence between the methods (e.g., running above the posterior cingulate sulcus in the left medial hemisphere and the right anterior insula in the right lateral hemisphere highlighted by white boxes). In other locations, a given parcellation method may identify features not revealed by the other (e.g., two area centers identified by RSFC-Snowballing [pointed out with white arrows] are surrounded by an area border defined by RSFC-Boundary Mapping on the lateral right hemisphere) encouraging the use of multiple methods for RSFC-based parcellation.

representation of area extent. Accordingly, just as it is important to focus on multiple modalities to accurately parcellate areas, it is advantageous to focus on multiple features that may distinguish areas (i.e., boundaries and centers or interiors).

RSFC-defined borders not only overlap with RSFC-defined system boundaries, but also reveal plausible areal divisions within the identified systems

Voxels can be clustered or grouped based on the similarity of their resting-state time series or their RSFC maps (e.g., using community detection, clustering algorithms, or independent component analysis (ICA)[5]; e.g., Doucet et al., 2011; Mumford et al., 2010; Power et al., 2011; Smith et al., 2009; Yeo et al., 2011). In some cases, the identified clusters have demonstrated a considerable degree of overlap with functionally defined systems, providing evidence that patterns of RSFC can be used to identify system-level organization (e.g., Power et al., 2011; Smith et al., 2009). Although many clustering approaches have been described as methods of parcellation, it is important to recognize that the purpose (and the outcome) of these analyses typically differs from the work presented here. Community detection, clustering, and component separation techniques operate on a data space that is blind to the underlying neuroanatomy. As a consequence, RSFC-based clustering techniques are capable of identifying collections of voxels or locations with similar properties, but these collections are not bound by space and may also group distinct adjacent areas into a single cluster. Accordingly, the majority of clustering analyses have typically identified locations that are functionally similar and may compose a given system (e.g., the visual system or the default system), but do not necessarily parcellate areas themselves (e.g., V1 versus V2 of the visual system). Direct comparisons of RSFC-defined system divisions and RSFC-based area parcellation provide illustrations of this important distinction.

RSFC clusters, communities, and components are not equivalent to areas

Brain systems are defined as groups of functionally related areas (Sejnowski and Churchland, 1989) and RSFC clustering techniques have identified collections of areas (or technically, regions/voxels) that likely represent functional brain systems at the scales that have been prominently explored. It is important to point out that the voxels corresponding to a given cluster are often spatially discontiguous, and can even span the length of the brain (e.g., groupings labeled as the default system typically include voxels in the medial prefrontal cortex and posterior parietal cortex; Fig. 7a). It should be clear based on this discontinuity alone that the identification of a cluster may reflect a granularity of organization that should not be confused with the parcellation of an area.

RSFC-defined area borders are consistent with RSFC-defined system boundaries in many locations

If clustering techniques are capable of identifying putative systems, and systems are composed of areas, the locations of system divisions should overlap with the locations of some areal boundaries. Fig. 7b depicts the correspondence between system divisions (i.e., transitions between two adjacent clusters) and the 120-subject RSFC-Boundary map. As expected, many locations that are system divisions exhibit high RSFC-Boundary Mapping edge probabilities. A direct comparison of RSFC-defined boundaries and two published systems maps (Power et al., 2011 and Yeo et al., 2011) was conducted. Fig. 7c depicts the distribution of edge probability values across all cortical vertices. Two separate distributions are presented in each histogram: the subset of edge probability values located at cortical vertices that were identified as system divisions (colored in yellow (Power et al., 2011) and orange (Yeo et al., 2011)), and the subset of edge probability values located at cortical vertices that were not identified as system divisions (colored in purple). Locations of system divisions exhibited higher edge probability values than the locations not identified as system divisions[6] (Power et al. (2011) division comparison: median edge probability at locations that are system divisions: 0.168, median edge probability at locations that are not system divisions: 0.144, $W(57034) = 492580832$, $z = 19.5$, $p < <0.0001$; Yeo et al. (2011) division comparison: median edge probability at locations that are system divisions: 0.174, median edge probability at locations that are not system divisions: 0.143, $W(57034) = 471727456$, $z = 28.0$, $p < <0.0001$).

RSFC-defined systems contain multiple areal divisions

The locations of putative system divisions revealed by clustering techniques coincide with the locations of several strong putative area boundaries as identified by RSFC-Boundary Mapping. One might try to use clustering techniques for parcellation by segregating a cluster into portions that only contain adjacent voxels or vertices and label these sub-clusters as areas. However, there is a strong reason to be cautious in this regard. As a prominent example, it should be apparent that this would result in the entire visual system in Fig. 8a (blue community) being labeled as a single area. Consistent with this, it is apparent that many locations not identified as system divisions exhibit high edge probability (RSFC boundary) likelihood (see purple bars in histograms depicted in Fig. 7c). These observations support the notion that system divisions are not a comprehensive representation of area boundaries.

Further comparison of RSFC-derived clusters and communities to RSFC-derived borders confirms that, in some cases, multiple strong boundaries can be found within a single contiguous portion of a cluster or community. We have already pointed out the parcellation of PA17/PA18 using RSFC-Boundary Mapping; here we highlight a portion of the left lateral inferior frontal cortex as an additional example of a location where multiple boundaries are observed within a cluster. Two independent techniques (community detection (yellow in Power et al., 2011) and clustering (orange in Yeo et al., 2011)) identified similar clusters of continuous voxels spanning the extent of the left inferior/middle frontal gyrus, a portion of the frontal-parietal control system (Fig. 7d). However, the RSFC-Boundary Mapping parcellation suggests the presence of 3 borders (corresponding to 4 putative areas, as defined by identifying the local-minima of the RSFC-Boundary Mapping map) within these clusters. While it is possible that the presence of RSFC-Boundary Mapping divisions simply reflect subtle and progressive distinctions within a single area, this would be inconsistent with the architectonic divisions that have been noted along this part of the brain (e.g., Brodmann's areas 44–47 and possibly 10). Furthermore, examination of the seed-based RSFC maps obtained from locations within each of these divisions suggests otherwise (the most posterior location (4) has an RSFC map most similar to the most anterior location (1), which are quite distinct from maps obtained from locations (2) and (3); Fig. 7e).

Why do clustering techniques behave differently than the RSFC-Boundary Mapping parcellation method highlighted here? Clustering techniques, for a given a priori or data-determined number of clusters, will identify groups of voxels that minimize RSFC similarity distance within clusters while simultaneously maximizing RSFC similarity distance between clusters. This focus on maximizing global separation may come at the cost of more local distinctions. In contrast, parcellation methods that rely on local feature changes (such as RSFC-Boundary Mapping) will be more sensitive to transitions in cortical identity (e.g.,

[5] While there are important differences across each of these methods, for simplicity we will refer to the collection of methods as 'clustering techniques' and the identified units as 'clusters'.

[6] Kolmogorov-Smirnov goodness-of-fit hypothesis tests revealed that the distributions of the RSFC-Boundary Mapping edge probabilities were non-normal and log transformation did not achieve normality. Accordingly, a Wilcoxon rank sum test was used to determine the probability with which the two distributions had equivalent medians.

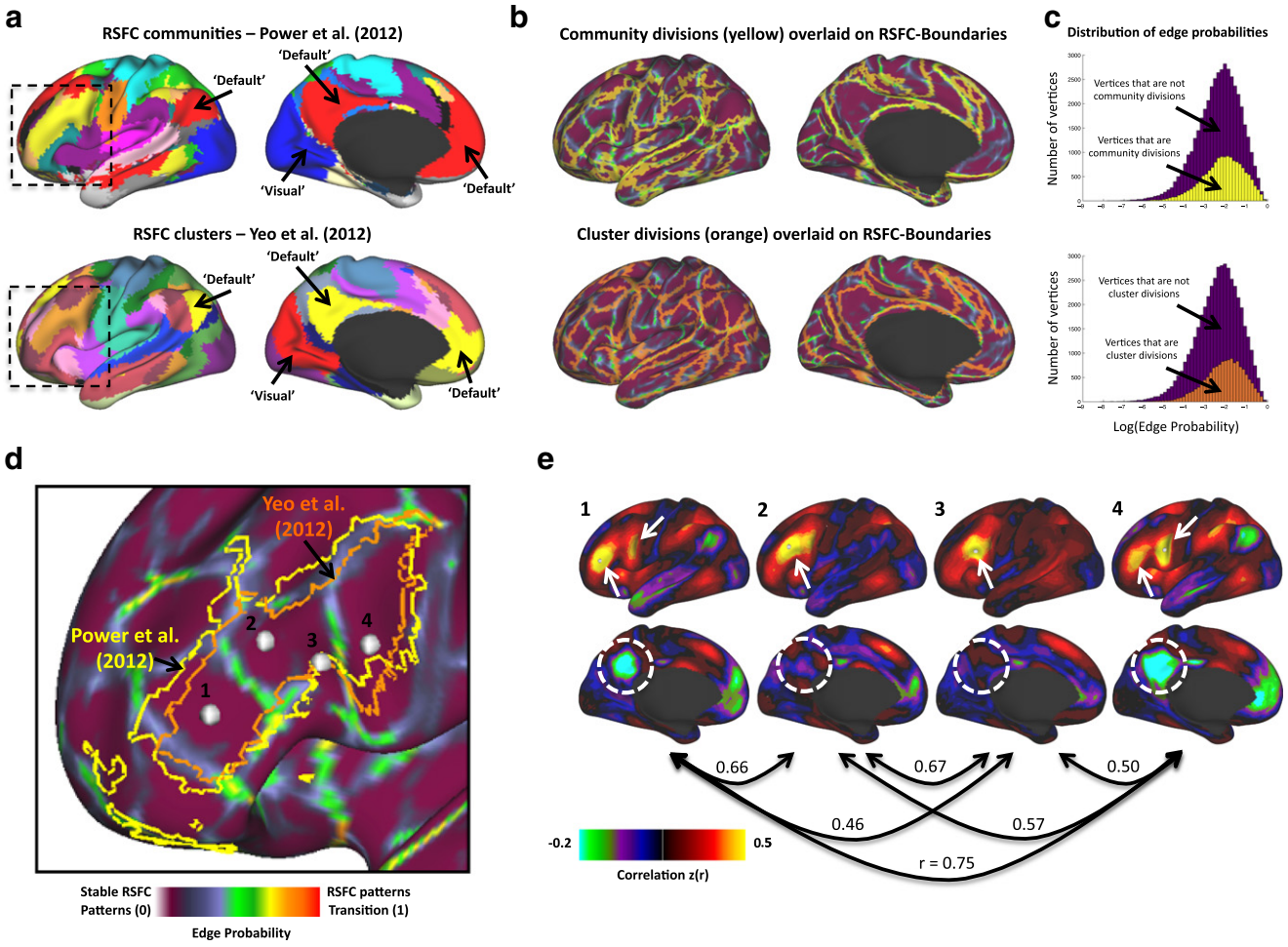

Fig. 7. RSFC-Boundary Mapping compared to RSFC-defined systems boundaries. (a) Large-scale cortical systems derived from RSFC community detection (Power et al., 2011) and clustering (Yeo et al., 2011). Dotted boxes indicate approximate view in (d). (b) RSFC-based system divisions (community divisions from Power et al., 2011; cluster divisions from Yeo et al., 2011) overlaid on a 120-subject RSFC-Boundary map depict the correspondence between the two types of maps. (c) Histograms depicting the distribution of edge probabilities for locations that were identified as system divisions as defined by Power et al. (yellow) and Yeo et al. (orange) and locations that were not identified as system divisions (purple in both). Note that system division edge probabilities are slightly right shifted relative to the edge probabilities of the remaining locations (i.e. tend to have higher edge probabilities), but there remain many locations with high edge probabilities that are not accounted for by system divisions. (d) close-up of left lateral frontal cortex showing frontal–parietal system borders overlaid on RSFC-Boundary map. Four white balls indicate local minima in the RSFC-Boundary map. (e) The spatial correlation (Pearson's r) between the four correlation maps generated from the local minima positions indicated in (d). Note that the most anterior (1) and most posterior (4) seeds have very similar correlation maps. The two intermediate seeds (2,3) show similar patterns as seeds 1 and 4, but also differ markedly in certain regions, e.g. along the lateral frontal cortex (arrows) and in posterior cingulate cortex (dotted circle), providing evidence that there are numerous areas within a single system division.

from V1 to V2 in Fig. 6). It may be possible for a clustering technique to identify a collection of voxels or vertices that corresponds to a single area if the method is invoked using both an appropriate level of granularity and with spatial constraints. However, complete partitioning at a given spatial scale (e.g., systems or areas) would require a perfectly hierarchical RSFC structure. The appropriate level of the RSFC hierarchy to define a given cortical area may be the same level that defines a system of areas elsewhere. As such, just as is the case with RSFC-Boundary Mapping, appropriate comparisons are necessary to understand the clustering observations further and ensure biological plausibility.

Additional constraints and considerations

While we have attempted to point out potential caveats and sources that require particular further attention, we highlight here additional considerations in the application of RSFC for area parcellation. Specifically, we focus on the relationship between RSFC-defined boundaries and BOLD signal strength and surface geometry, and also make some comments on parcellation of subcortical structures using patterns of RSFC.

Relationship of RSFC-defined borders to BOLD signal strength

It is important to note that observed transitions in the patterns of RSFC may not be neurobiologically relevant. In particular, boundaries that correspond to BOLD signal differences relating to variable BOLD sensitivity across the brain (e.g. due to magnetic field inhomogeneities arising from adjacent structures with different magnetic susceptibilities Frahm et al., 1988) are likely of little interest in the context of cortical parcellation. With this in mind, we compared the RSFC-Boundary maps to the BOLD signal strength across the brain. Mean BOLD signal was calculated by averaging the first frame of acquisition (post-steady state magnetization) from all subjects (Ojemann et al., 1997). A small positive correlation ($r = 0.12$) was found between the change in the mean BOLD signal along the cortical surface (measured by the gradient, or spatial derivative, of the mean BOLD signal) and the 120-subject RSFC-Boundary map. BOLD signal strength changes may account for a small amount of variability in the RSFC-Boundary map, but even this may be largely confined to regions known to have significant signal loss. Fig. 8a depicts the pattern of BOLD signal dropout in our data. BOLD data was normalized to a mode of 1000 during preprocessing. Accordingly, a mean BOLD signal of 800 or less (depicted in orange shades)

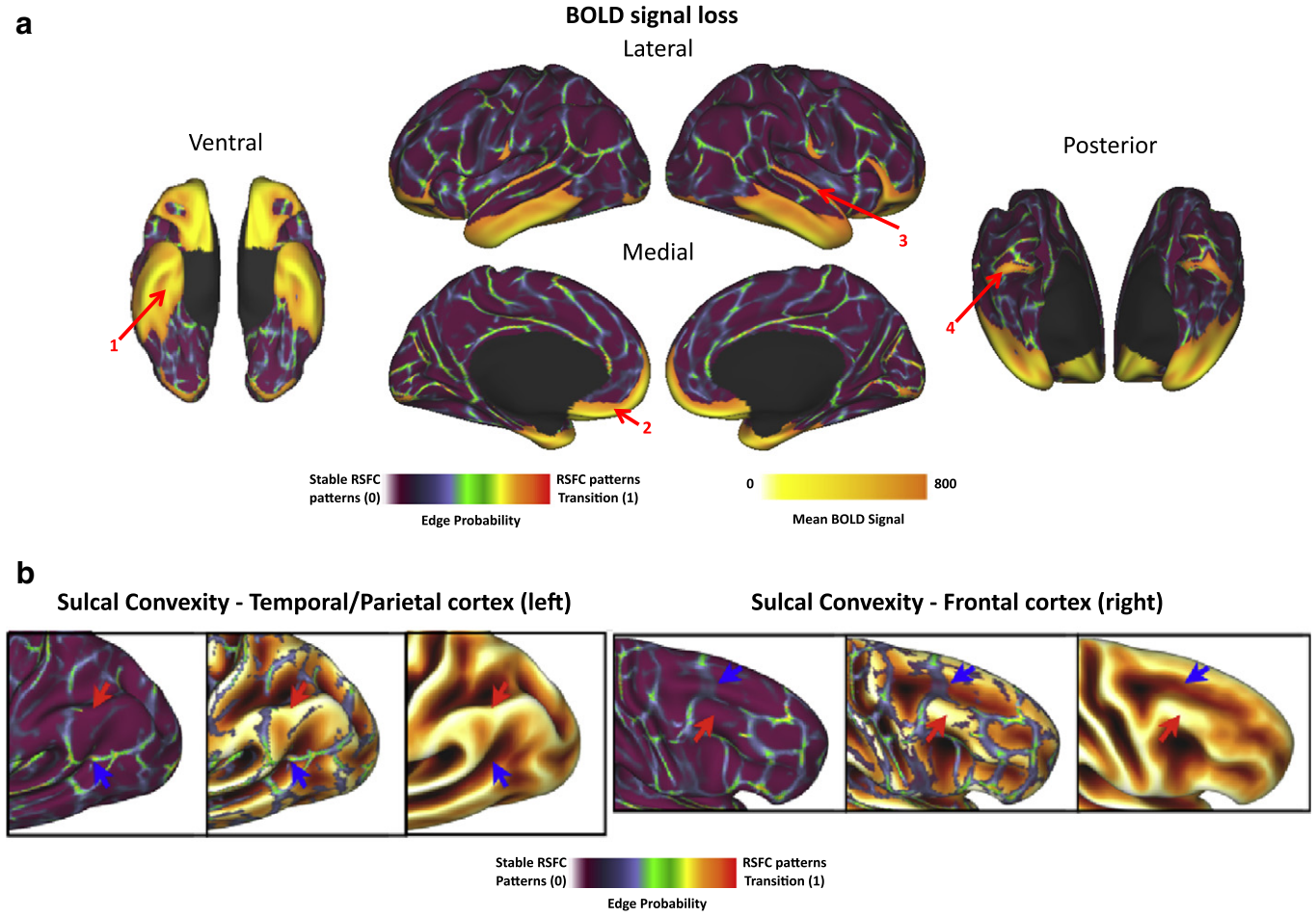

Fig. 8. RSFC-Boundary Mapping compared to BOLD signal strength and surface geometry. (a) Mean BOLD signal from the first frame of resting state data from 120 subjects overlaid on RSFC-Boundary map. Regions with BOLD signal less than 800 (BOLD signal has been mode 1000 normalized) can be seen in orange-yellow. Signal loss is apparent in ventral temporal (red arrow '1') and orbitofrontal (red arrow '2') regions, superior temporal gyrus (red arrow '3'), and the occipital pole (red arrow '4'). (b) Lateral parietal–occipital (right) and lateral frontal views of RSFC-Boundary map compared to surface geometry. Left panels show full range RSFC-Boundary map, middle panels show RSFC-Boundary map thresholded at 0.15 boundary frequency, and right panels show average surface convexity of Conte-69 atlas (darker and brighter values on this surface represent sulcal and gyral regions respectively). Red arrows indicate gyral crowns where there is an absence of a strong RSFC-defined border and blue arrows indicate regions in which RSFC boundaries cross over sulcal fundi.

represents a substantial attenuation of signal. Boundaries in the ventral portion of the temporal lobe (red arrow 1) and in orbitofrontal cortex (red arrow 2) are clearly suspect given the large signal loss in these regions. Similarly, the boundaries along the superior temporal gyrus (red arrow 3) and at the occipital pole (red arrow 4) may be explained by the decreased signal in these regions. Leaving out regions with substantial signal loss (i.e. BOLD <800) significantly reduces the correlation between the change in BOLD signal strength and the RSFC-Boundary map ($r = 0.07$). We conclude that for much of the brain changes in BOLD signal strength do not account for the presence of RSFC-defined boundaries. Field map-based distortion correction, which was not carried out here as many subjects in our cohort had not been collected with field maps, may help ameliorate distortion-related effects, but would not be able to repair boundaries related to frank signal loss. Consideration of artifacts such as these are critical to keep in mind when interpreting boundaries and highlight regions of the brain where RSFC-based tools will struggle to generate meaningful parcellation without further processing or acquisition refinements.

Relationship of RSFC-defined borders to surface geometry

Areal borders need not respect morphometric divisions. For example, the primary visual area (V1) spans both sides of the calcarine sulcus, reflecting the upper and lower representations of the visual field in this area (e.g., Dougherty et al., 2003). However, a number of strong borders defined by RSFC-Boundary Mapping follow prominent gyral and sulcal landmarks: strong RSFC borders are present along the central sulcus (from dorsal to ventral) and along the cingulate gyrus (from anterior to posterior). While some of these divisions may be consistent with areal divisions (e.g., the primary motor and somatosensory areas follow the central sulcus along the pre- and post-central gyri, respectively), one concern is that the identification of RSFC-Boundary Mapping borders is biased by surface geometry (for example, as a consequence of the volume-to-surface processing and analysis stream; see methods in Appendix A — Methods). Indeed, the RSFC-Boundary map has a small positive correlation with the average convexity of the Conte69 atlas ($r = 0.11$). A number of observations mitigate this concern however. Fig. 8b highlights a few examples in the frontal and temporal/parietal cortex where strong RSFC boundaries are not found along gyral crowns (red arrows), as well as examples of regions where strong RSFC boundaries cross over sulcal fundi (blue arrows). While it is conceivable that RSFC borders follow morphometric landmarks in some locations as a consequence of the presence of an areal division, we do not view gyral and sulcal features as the causal source of group-level RSFC borders. We recognize that the previous observations do not completely rule out the possibility that inter-individual variability in surface geometry may be masked when individuals are combined into a group, and that geometric bias may be present when RSFC borders are computed on individual subjects. With respect to the latter point, observations in our laboratory suggest otherwise (e.g., see Supplemental Fig. 3 in Wig et al., 2013).

RSFC-based parcellation of subcortical structures

While we have focused our present discussions on parcellation of cortical areas, many of the general points we have made are applicable to subdividing subcortical structures, with some caveats. For example, the gradient-based approach described here is applied primarily for the 2-dimensional parcellation of the cortical sheet; subcortical structures, however, are not arrayed on a sheet, but rather are organized as nuclei having, sometimes complex, 3-dimensional forms. As such, different approaches are necessary for their parcellation. The gradient-based strategy for finding RSFC pattern transitions can naturally be extended into 3-dimensions for this purpose, though we do not present such an approach here. The current form of the RSFC-Snowballing procedure is not limited to the cortical surface and is capable of identifying area centers within subcortical structures, which in fact is highlighted elsewhere (Wig et al., 2013). In addition, clustering approaches have clearly demonstrated the ability to partition subcortical structures according to RSFC correlations (e.g., Barnes et al., 2010; Zhang et al., 2008). As with the cortex, much work remains to be done comparing apparent RSFC-based distinctions with other modalities to understand how RSFC information in the subcortical nuclei and the cerebellum converges with and/or diverges from other properties of brain organization and function.

Concluding comments

Patterns of RSFC exhibit abrupt transitions across the brain and recent advances in BOLD imaging acquisition and analysis have facilitated the development of tools to map the locations of these changes across the cortical surface. Throughout this report, we have described some prominent observations where the locations of putative areal divisions as defined by RSFC-Boundary Mapping converge with features from other parcellation modalities as well as other RSFC analysis methods.

Where possible, we have attempted to highlight observations and issues that necessitate particular attention in order to more fully understand and interpret the parcellation information gleaned from RSFC-based approaches. Of course, as the nature and source of RSFC signals is continually explored, we suspect our understanding of RSFC-based area parcellation will also be modified. For example, deeper understanding of the non-stationary nature of RSFC signals (e.g., Chang and Glover, 2010; Smith et al., 2012) and of the sensitivity of RSFC to various sources of spurious noise (e.g., Birn et al., 2006; Chang et al., 2009; Power et al., 2012; Satterthwaite et al., 2012; Van Dijk et al., 2012), as well as improved image acquisition and processing techniques (De Martino et al., 2011; Van Essen et al., 2012) will likely aid our ability to use RSFC for parcellating cortical and subcortical areas.

The parcellation of brain areas relies on distinctions related to function, architectonics, connectivity and topography. While the earliest parcellation of human cortical areas relied on invasive approaches such as post-mortem dissection (e.g., Brodmann, 1909; Vogt and Vogt, 1919) or intra-cranial recording (e.g., Jasper and Penfield, 1954), recent advances in brain imaging have enabled continual improvements and refinement in our understanding of the properties and methods for identifying areal divisions (Toga et al., 2006; the present special issue on *In vivo Brodmann mapping in neuroimage*). As has been the case with parcellation of non-human cortical areas, it is likely that no single feature will serve to parcellate all cortical and subcortical structures. Accurate and informative parcellation has been accomplished by the careful consideration of multiple converging features. In additional to distinctions identified by examining patterns of evoked-activity, connectional anatomy, architectonics, and topography, we feel there is sufficient and compelling evidence to suggest that patterns of RSFC provide confirmatory and complementary information for the purposes of parcellating cortical areas and subcortical divisions of the brain. We urge interested readers to explore and utilize our RSFC-based parcellation maps for themselves, we have made these maps available on our laboratory website (http://www.nil.wustl.edu/labs/petersen/Publications.html).

Acknowledgments

We thank Alex Cohen, Steven Nelson, Jonathan Power, and Brad Schlaggar for thoughtful discussions and feedback throughout much of this work. We also thank Malcolm Tobias, Avi Snyder, Matt Glasser, and Babatunde Adeyemo for technical support and assistance. This work was supported by a McDonnell Foundation Collaborative Action Award, NIH (32979, 46424, 61144) and the Human Connectome Project (1U54MH091657) from the 16 NIH Institutes and Centers that support the NIH Blueprint for Neuroscience Research.

Appendix A. Methods

Subjects

RSFC from a total of 120 healthy young adult subjects was analyzed for parcellation (60 females, mean age = 25 years, age range = 19–32 years). All subjects were native speakers of English and were right-handed. Subjects were recruited from the Washington University community and were screened with a self-report questionnaire to ensure that they had no current or previous history of neurological or psychiatric diagnosis. Informed consent was obtained from all subjects. The study was approved by the Washington University School of Medicine Human Studies Committee and Institutional Review Board.

Data acquisition parameters

Structural and RSFC (functional) MRI data were obtained with a Siemens Magnetom Trio Tim 3.0 T Scanner (Erlangen, Germany) and a Siemens 12 channel Head Matrix Coil. To help stabilize head position, each subject was fitted with a thermoplastic mask fastened to holders on the headcoil. A T1-weighted sagittal magnetization-prepared rapid acquisition gradient echo (MP-RAGE) structural image was obtained (TE = 3.08 ms, TR(partition) = 2.4 s, TI = 1000 ms, flip angle = 8°, 176 slices with $1 \times 1 \times 1$ mm voxels) (Mugler and Brookeman, 1990). An auto align pulse sequence protocol provided in the Siemens software was used to align the acquisition slices of the functional scans parallel to the anterior commissure–posterior commissure (AC–PC) plane and centered on the brain. This plane is parallel to the slices in the Talairach atlas (Talairach and Tournoux, 1988).

During RSFC data acquisition, subjects were instructed to relax while fixating on a black crosshair that was presented against a white background. Functional imaging was performed using a blood oxygenation level-dependent (BOLD) contrast sensitive gradient echo echo-planar sequence (TE = 27 ms, flip angle = 90°, in-plane resolution = 4×4 mm). Whole brain EPI volumes (MR frames) of 32 contiguous, 4 mm-thick axial slices were obtained every 2.5 s. A T2-weighted turbo spin echo structural image (TE = 84 ms, TR = 6.8 s, 32 slices with $1 \times 1 \times 4$ mm voxels) in the same anatomical planes as the BOLD images was also obtained to improve alignment to an atlas. The number of volumes obtained from subjects ranged from 184 to 729 (mean = 336 frames).

Image preprocessing

Functional images were first processed to reduce artifacts (Miezin et al., 2000). These steps included: (i) correction of odd vs. even slice intensity differences attributable to interleaved acquisition without gaps, (ii) correction for head movement within and across runs and (iii) across-run intensity normalization to a whole brain mode value of 1000. Atlas transformation of the functional data was computed for each individual using the MP-RAGE scan. Each run was then re-

sampled to an isotropic 3-mm atlas space (Talairach and Tournoux, 1988), combining movement correction and atlas transformation in a single cubic spline interpolation (Lancaster et al., 1995; Snyder, 1996). This single interpolation procedure avoids blurring that would be introduced by multiple interpolations. All subsequent operations were performed on the atlas-transformed volumetric time series.

RSFC preprocessing

Several additional preprocessing steps were utilized to reduce spurious variance unlikely to reflect neuronal activity in RSFC data. RSFC preprocessing was performed in two iterations. In the first iteration, RSFC preprocessing included, in the following order: (i) multiple regression of the BOLD data to remove variance related to the whole brain signal (cf. Scholvinck et al., 2010), ventricular signal, white matter signal, six detrended head realignment parameters obtained by rigid body head motion correction, and the first-order derivative terms for all aforementioned nuisance variables. (ii) A band-pass filter ($0.009\ Hz < f < 0.08\ Hz$), (iii) volumetric spatial smoothing (6 mm full width at half maximum in each direction).[7]

Following the initial RSFC preprocessing iteration, to ameliorate the effect of motion artifact on RSFC correlations, data was processed following the recently described 'scrubbing' procedure (Power et al., 2012). Temporal masks were created to flag motion-contaminated frames so that they could be ignored during subsequent nuisance regression and correlation calculations. Motion contaminated volumes were identified by frame-by-frame displacement (FD, calculated as the sum of absolute values of the differentials of the 3 translational motion parameters and 3 rotational motion parameters) and by frame-by-frame signal change (DVARS). Volumes with FD >0.3 mm or DVARS >3% signal change were flagged. In addition, the two frames acquired immediately prior to each of these frames and the two frames acquired immediately after these frames were also flagged to account for temporal spread of artifactual signal resulting from the temporal filtering in the first RSFC preprocessing iteration.

The RSFC preprocessing steps outlined above (steps i–iii; including nuisance regression, temporal filtering, and volumetric smoothing) were applied in the second iteration on RSFC data that excluded volumes flagged during motion scrubbing. The mean percent of frames excluded from the remaining subjects was 26% (range: 1%–26.0%). All subjects had a minimum of 126 frames remaining after RSFC preprocessing (mean = 245 frames).

Surface preprocessing

Following volumetric registration, each subject's MP-RAGE image was processed to generate anatomical surfaces using FreeSurfer's default recon-all processing pipeline (version 5.0). This pipeline included brain extraction, segmentation, generation of white matter and pial surfaces, inflation of the surfaces to a sphere, and surface shape-based spherical registration of the subject's 'native' surface to the fsaverage surface (Dale and Sereno, 1993; Dale et al., 1999; Fischl et al., 1999; Ségonne et al., 2004, 2005). The fsaverage-registered left and right hemisphere surfaces were brought into register with each other using deformation maps from a landmark-based registration of the left and right fsaverage surfaces to a hybrid left–right fsaverage surface ('fs_LR'; Van Essen et al., 2012) and resampled to a resolution of 164,000 vertices (164k fs_LR) using Caret tools (Van Essen et al., 2001). Finally, each subject's 164k fs_LR surface was down-sampled to a 32,492 vertex surface (fs_LR 32k), which allowed for analysis in a computationally tractable space while still oversampling the underlying resolution of BOLD data used in subsequent analyses. The various deformations from the 'native' surfaces to the fs_LR 32k surface were composed into a single deformation map allowing for one step resampling. The above procedure results in a surface space that allows for quantitative analysis across subjects as well as between hemispheres. A script for this procedure is available on the Van Essen Lab website (Freesurfer_to_fs_LR Pipeline, http://brainvis.wustl.edu).

RSFC-Boundary Mapping

RSFC-Boundary Mapping identifies transitions in resting state correlations across the cortical surface. Cohen et al.'s (2008) original approach applied 2-D image processing tools to BOLD data sampled from patches on a flattened cortical surface (e.g., Nelson et al., 2010a). Flattening the surface induces distortions in the surface representation that could lead to spurious boundary identification. The current implementation of RSFC-Boundary Mapping avoids this issue by performing all computations directly on a closed surface topology. The analysis is now also applied to the entire cortical surface as opposed to small selected patches of cortex. The details of this procedure have been described for individual subjects elsewhere (Wig et al., 2013). Here we apply the method to groups of individuals.

A flowchart of the RSFC-Boundary Mapping procedure can be seen in Fig. 9. The RSFC BOLD time courses[8] were first sampled to each subject's individual 'native' midthickness surface (generated as the average of the white and pial surfaces) using the ribbon-constrained sampling procedure available in Connectome Workbench 0.7. This procedure samples data from voxels within the gray matter ribbon (i.e. between the white and pial surfaces) that lay in a cylinder orthogonal to the local midthickness surface weighted by the extent to which the voxel falls within the ribbon — it is designed to minimize partial-volume effects arising from the low sampling resolution of the BOLD data relative to the structural image acquisition (Glasser and Van Essen, 2011). Once sampled to the 'native' surface, the time courses were smoothed along the surface using a Gaussian smoothing kernel ($\sigma = 2.55$). The smoothed time courses were deformed and resampled from the individual's 'native' surface to the 32k fs_LR surface in a single step using the deformation map generated as described above.

Each surface vertex's time course was correlated with the time courses from every voxel in a brain mask to generate full volume correlation maps (32,492 vertices × 65,549 voxels). Each correlation map was transformed using Fisher's r-to-z transformation (Zar, 1996) and averaged across subjects. Full volume correlation maps were used instead of surface correlation maps in order to ensure that sub-cortical correlation relationships contributed to areal parcellation. An RSFC map similarity matrix was created by calculating the spatial correlation between every vertex's RSFC correlation maps with one another, producing a 32k × 32k matrix. Each row of this matrix corresponds to a map on the cortical surface wherein the values reflect the similarity of a given vertex RSFC map with the RSFC map of every other vertex. To find positions where RSFC similarity exhibited abrupt changes, the similarity maps were first Gaussian smoothed along the surface ($\sigma = 2.55$) and the first spatial derivative was computed using the 'metric-gradient-all' function available in Caret 5.65. This resulted in 32k 'gradient' maps for each hemisphere. These gradient maps represent the essential feature of RSFC transition we aim to identify. As a further refinement relative to whole-brain boundary maps presented in previous work (Wig et al., 2013), in order to sharpen observed borders and facilitate identification of even subtle differences in correlation patterns, we applied a non-maxima suppression procedure to each of the gradient maps, creating 32k 'edge' maps. This technique identifies a vertex as an edge if it is a gradient maxima with respect to at least two pairs of spatially non-adjacent neighboring vertices (each of the 32k vertices has six neighbors, except 12 which have five neighbors). The non-linear nature of this step

[7] Volumetric smoothing was only performed as an RSFC preprocessing step for RSFC-Snowballing.

[8] No spatial smoothing was performed in the volume during pre-processing for RSFC-Boundary Mapping so as to minimize any partial-volume effects and cross-sulcal data blurring.

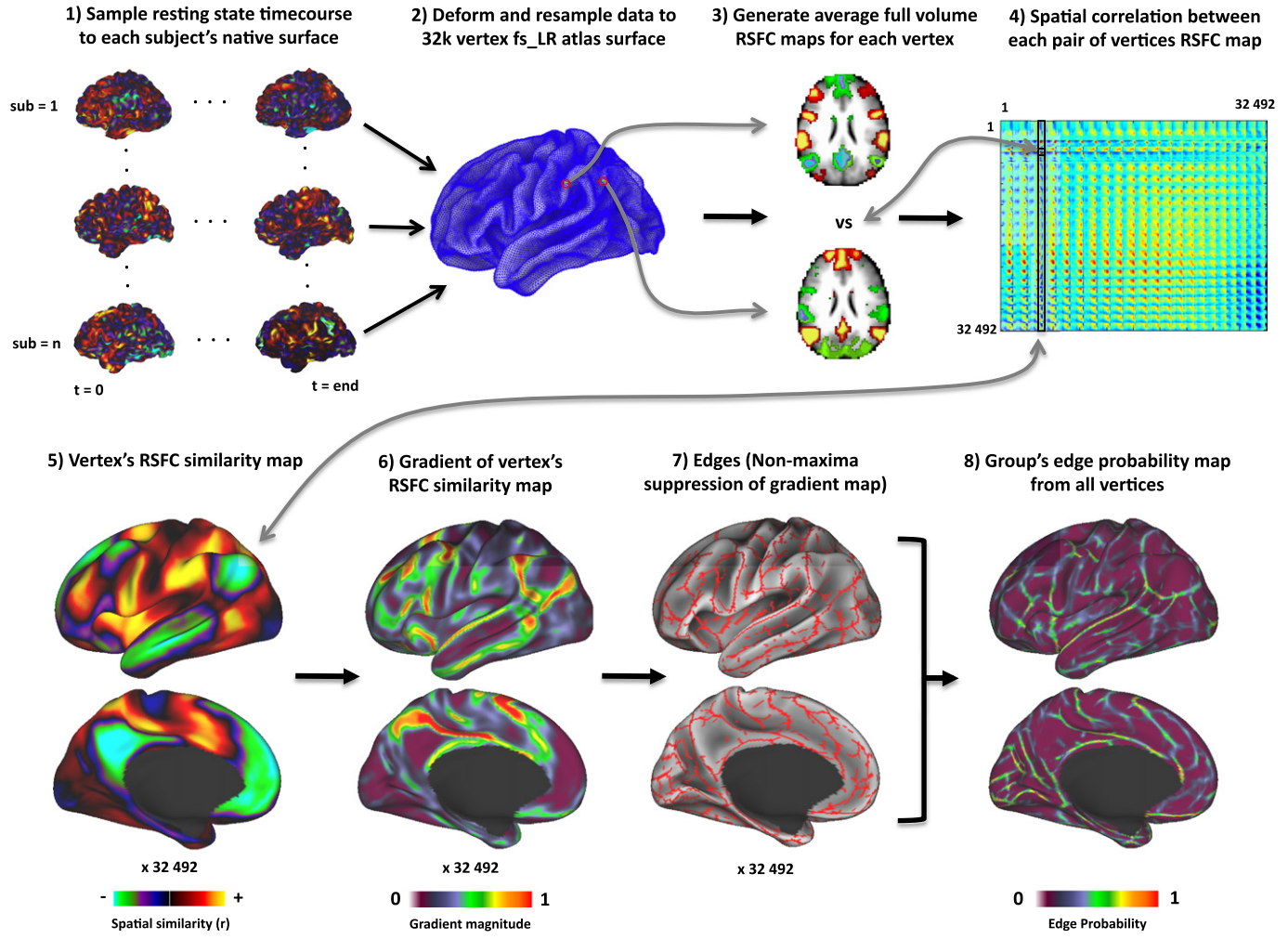

Fig. 9. RSFC-Boundary Mapping procedure. (1) Resting state time courses are first sampled to each subject's native midthickness surface and smoothed along the surface. (2) The sampled data is then deformed and resampled to the 32k fs_LR surface space (Van Essen et al., 2012). (3) Full volume RSFC maps are calculated for all surface vertices and averaged across all subjects. (4) The spatial correlation between all RSFC maps is calculated generating a 32,492 × 32,492 vertex matrix. (5) Each column of this matrix represents each surface vertex's RSFC similarity map. (6) The spatial gradient of each RSFC similarity map is computed. (7) Edges in the gradient map are highlighted by non-maxima suppression (where 1 indicates an edge and 0 indicates no edge). (8) Finally, the edge maps from all vertices are averaged together; this generates a final RSFC-Boundary map that indicates how frequently an edge was detected at each vertex (edge probability).

makes it susceptible to potentially uninteresting noise in the input data; averaging correlation maps from many subjects minimizes this possibility. Finally, the 32k 'edge' maps from each hemisphere were averaged to indicate the frequency with which a given vertex was identified as an edge.

RSFC-Snowball sampling

RSFC-Snowball sampling (RSFC-Snowballing) identifies locations that exhibit a high density of resting-state correlations to other locations in the brain. Peak density values are lesser at locations that are transition points (or boundaries) between adjacent areas and greater within an area's interior (or center). Therefore, the voxel-wise distribution of peaks can be used to identify the locations of area centers. A separate report describes RSFC-Snowballing for parcellating cortical and sub-cortical structures in an individual subject (Wig et al., 2013). As with RSFC-Boundary Mapping, we describe here the method for application to groups of individuals.

RSFC-Snowballing is an iterative procedure that uses seed-based RSFC to identify locations correlated with a starting seed location (i.e., the 'neighbors' of the seed, in a graph theoretic sense), and then identifies the neighbors of the neighbors, and so forth over multiple iterations (zones). RSFC-Snowballing is initialized from multiple starting seed locations (i.e., from a pre-defined set of coordinates) creating a peak density map for each starting location. The peak density maps derived from each starting location are summed and normalized relative to the maximum value of the summed map to arrive at an aggregate peak density map (Fig. 10). In the present analysis, the starting location set was defined from a meta-analysis of task-evoked data, which identified 151 task-defined centers across cortical and sub-cortical structures (for details see Wig et al., 2013). Aggregating the peak density maps from multiple starting locations minimizes the potential bias of a single starting seed location and provides estimates of area centers across broad expanses of the brain's cortical and subcortical structures.

A neighbor of a given seed need not be physically adjacent to the seed, but rather is defined by the presence of an RSFC relationship above a given correlation threshold. Neighbor identification was conducted by calculating seed-based statistical correlation maps across the group of individuals. For each participant, the average time course was extracted from the seed region of interest (ROI) and Pearson's correlation coefficient was computed between this ROI's time course and the time course for each voxel across the whole brain volume. The resulting correlation map was converted to z values using Fisher's r-to-z transformation (Zar, 1996). The individual z(r) images were

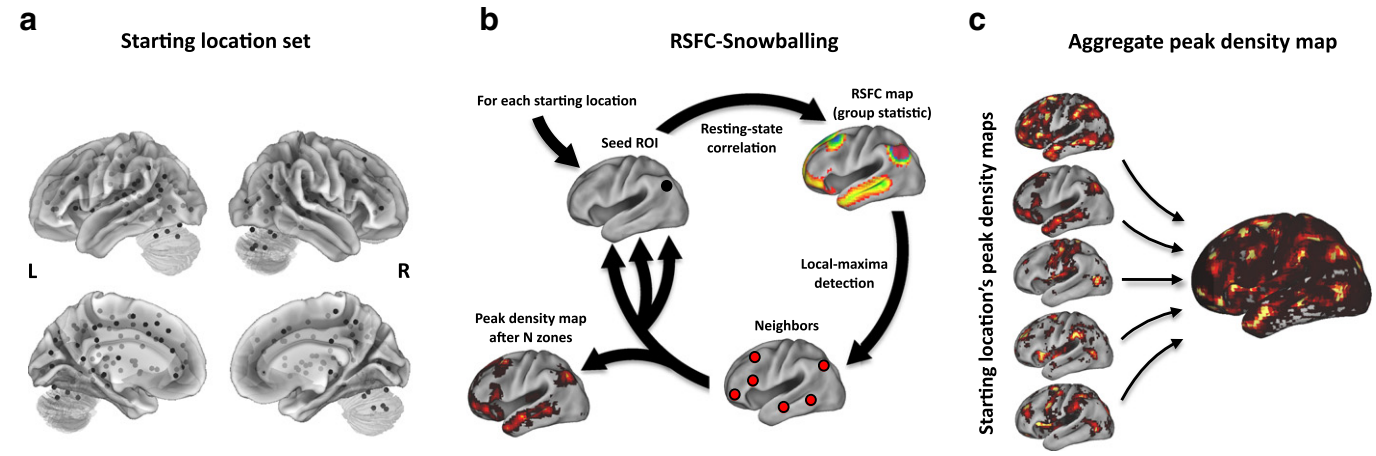

Fig. 10. Overview of RSFC-Snowballing using multiple starting seed locations. (a) Initialization location set consisting of cortical and sub-cortical seed locations (n = 151) defined by meta-analysis of task-evoked data. (b) For each seed location in the initialization location set, RSFC-Snowballing iteratively identifies the neighbors (peaks of RSFC correlation) of seed ROIs over multiple zones and adds these neighbors to a peak density map. (c) The independently derived peak density maps from each of the seed locations of the initialization location set are summed to arrive at an aggregate peak density map presumed to reflect the likelihood with which a given location is an area center.

next submitted to a random-effects analysis, treating participant as the random factor, to create a statistical map using a t-test. To identify the seed ROI's 'neighbors' (i.e. the regions that were correlated with the seed ROI), the statistical t-maps were first smoothed (6 mm FWHM) and the local maxima (peaks) of contiguous clusters of voxels that both surpassed a correlation threshold ($p < 0.001$, uncorrected) and had a minimum distance of 10 mm between peaks were identified.

Each starting location was submitted to RSFC-Snowballing over 3 zones. The final aggregate peak density map was spatially smoothed (volumetric smoothing of 6 mm FWHM) and then normalized relative to its maximal value to facilitate viewing.

Conflict of interest

The authors declare no conflict of interest.

References

Amunts, K., Malikovic, A., Mohlberg, H., Schormann, T., Zilles, K., 2000. Brodmann's areas 17 and 18 brought into stereotaxic space—where and how variable? NeuroImage 11, 66–84.

Amunts, K., Weiss, P.H., Mohlberg, H., Pieperhoff, P., Eickhoff, S., Gurd, J.M., Marshall, J.C., Shah, N.J., Fink, G.R., Zilles, K., 2004. Analysis of neural mechanisms underlying verbal fluency in cytoarchitectonically defined stereotaxic space—the roles of Brodmann areas 44 and 45. NeuroImage 22, 42–56.

Barnes, K.A., Cohen, A.L., Power, J.D., Nelson, S.M., Dosenbach, Y.B., Miezin, F.M., Petersen, S.E., Schlaggar, B.L., 2010. Identifying basal ganglia divisions in individuals using resting-state functional connectivity MRI. Front. Syst. Neurosci. 4, 18.

Barnes, K.A., Nelson, S.M., Cohen, A.L., Power, J.D., Coalson, R.S., Miezin, F.M., Vogel, A.C., Dubis, J.W., Church, J.A., Petersen, S.E., Schlaggar, B.L., 2012. Parcellation in left lateral parietal cortex is similar in adults and children. Cereb. Cortex 22 (5), 1148–1158 (May).

Birn, R.M., Diamond, J.B., Smith, M.A., Bandettini, P.A., 2006. Separating respiratory-variation-related fluctuations from neuronal-activity-related fluctuations in fMRI. NeuroImage 31, 1536–1548.

Biswal, B., Yetkin, F.Z., Haughton, V.M., Hyde, J.S., 1995. Functional connectivity in the motor cortex of resting human brain using echo-planar MRI. Magn. Reson. Med. 34, 537–541.

Biswal, B.B., Mennes, M., Zuo, X.N., Gohel, S., Kelly, C., Smith, S.M., Beckmann, C.F., Adelstein, J.S., Buckner, R.L., Colcombe, S., Dogonowski, A.M., Ernst, M., Fair, D., Hampson, M., Hoptman, M.J., Hyde, J.S., Kiviniemi, V.J., Kotter, R., Li, S.J., Lin, C.P., Lowe, M.J., Mackay, C., Madden, D.J., Madsen, K.H., Margulies, D.S., Mayberg, H.S., McMahon, K., Monk, C.S., Mostofsky, S.H., Nagel, B.J., Pekar, J.J., Peltier, S.J., Petersen, S.E., Riedl, V., Rombouts, S.A., Rypma, B., Schlaggar, B.L., Schmidt, S., Seidler, R.D., G, J.S., Sorg, C., Teng, G.J., Veijola, J., Villringer, A., Walter, M., Wang, L., Weng, X.C., Whitfield-Gabrieli, S., Williamson, P., Windischberger, C., Zang, Y.F., Zhang, H.Y., Castellanos, F.X., Milham, M.P., 2010. Toward discovery science of human brain function. Proc. Natl. Acad. Sci. U. S. A. 107, 4734–4739.

Brodmann, K., 1909. Vergleichende lokalisationslehre der grosshirnrinde in ihren prinzipien dargestellt auf grund des zellenbaues. J.A. Barth, Leipzig.

Carmichael, S.T., Price, J.L., 1994. Architectonic subdivision of the orbital and medial prefrontal cortex in the macaque monkey. J. Comp. Neurol. 346, 366–402.

Carmichael, S.T., Price, J.L., 1996. Connectional networks within the orbital and medial prefrontal cortex of macaque monkeys. J. Comp. Neurol. 371, 179–207.

Caspers, S., Geyer, S., Schleicher, A., Mohlberg, H., Amunts, K., Zilles, K., 2006. The human inferior parietal cortex: cytoarchitectonic parcellation and interindividual variability. NeuroImage 33, 430–448.

Chang, C., Glover, G.H., 2010. Time–frequency dynamics of resting-state brain connectivity measured with fMRI. NeuroImage 50, 81–98.

Chang, C., Cunningham, J.P., Glover, G.H., 2009. Influence of heart rate on the BOLD signal: the cardiac response function. NeuroImage 44, 857–869.

Cohen, A.L., Fair, D.A., Dosenbach, N.U., Miezin, F.M., Dierker, D., Van Essen, D.C., Schlaggar, B.L., Petersen, S.E., 2008. Defining functional areas in individual human brains using resting functional connectivity MRI. NeuroImage 41, 45–57.

Dale, A.M., Sereno, M.I., 1993. Improved localization of cortical activity by combining EEG and MEG with cortical surface reconstruction: a linear approach. J. Cogn. Neurosci. 5, 162–176.

Dale, A.M., Fischl, B., Sereno, M.I., 1999. Cortical surface-based analysis. I. Segmentation and surface reconstruction. NeuroImage 9, 179–194.

De Martino, F., Esposito, F., van de Moortele, P.F., Harel, N., Formisano, E., Goebel, R., Ugurbil, K., Yacoub, E., 2011. Whole brain high-resolution functional imaging at ultra high magnetic fields: an application to the analysis of resting state networks. NeuroImage 57, 1031–1044.

Deco, G., Jirsa, V.K., McIntosh, A.R., 2011. Emerging concepts for the dynamical organization of resting-state activity in the brain. Nat. Rev. Neurosci. 12, 43–56.

Deen, B., Pitskel, N.B., Pelphrey, K.A., 2011. Three systems of insular functional connectivity identified with cluster analysis. Cereb. Cortex 21, 1498–1506.

Dick, F., Tierney, A.T., Lutti, A., Josephs, O., Sereno, M.I., Weiskopf, N., 2012. In vivo functional and myeloarchitectonic mapping of human primary auditory areas. J. Neurosci. 32, 16095–16105.

Doucet, G., Naveau, M., Petit, L., Delcroix, N., Zago, L., Crivello, F., Jobard, G., Tzourio-Mazoyer, N., Mazoyer, B., Mellet, E., Joliot, M., 2011. Brain activity at rest: a multiscale hierarchical functional organization. J. Neurophysiol. 105, 2753–2763.

Dougherty, R.F., Koch, V.M., Brewer, A.A., Fischer, B., Modersitzki, J., Wandell, B.A., 2003. Visual field representations and locations of visual areas V1/2/3 in human visual cortex. J. Vis. 3, 586–598.

Fedorenko, E., Hsieh, P.J., Nieto-Castanon, A., Whitfield-Gabrieli, S., Kanwisher, N., 2010. New method for fMRI investigations of language: defining ROIs functionally in individual subjects. J. Neurophysiol. 104, 1177–1194.

Felleman, D.J., Van Essen, D.C., 1991. Distributed hierarchical processing in the primate cerebral cortex. Cereb. Cortex 1, 1–47.

Fischl, B., Sereno, M.I., Dale, A.M., 1999. Cortical surface-based analysis. II: Inflation, flattening, and a surface-based coordinate system. NeuroImage 9, 195–207.

Fischl, B., Rajendran, N., Busa, E., Augustinack, J., Hinds, O., Yeo, B.T., Mohlberg, H., Amunts, K., Zilles, K., 2008. Cortical folding patterns and predicting cytoarchitecture. Cereb. Cortex 18, 1973–1980.

Foerster, O., 1936. The motor cortex of man in light of Hughlings Jackson's doctrines. Brain 58, 135–159.

Fox, M.D., Raichle, M.E., 2007. Spontaneous fluctuations in brain activity observed with functional magnetic resonance imaging. Nat. Rev. Neurosci. 8, 700–711.

Frahm, J., Merboldt, K.D., Hanicke, W., 1988. Direct FLASH MR imaging of magnetic field inhomogeneities by gradient compensation. Magn. Reson. Med. 6, 474–480.

Gennari, F., 1782. Francisci Gennari Parmensis Medicinae Doctoris Collegiati de Peculiari Structura Cerebri Nonnullisque Eius Morbis-Paucae Aliae Anatom. Observat. Accedunt. Regio Typographeo, Parma, Italy.

Glasser, M.F., Van Essen, D.C., 2011. Mapping human cortical areas in vivo based on myelin content as revealed by T1- and T2-weighted MRI. J. Neurosci. 31, 11597–11616.

Goodman, L., 1961. Snowball sampling. Ann. Math. Stat. 32, 148–170.
Goulas, A., Uylings, H.B., Stiers, P., 2012. Unravelling the intrinsic functional organization of the human lateral frontal cortex: a parcellation scheme based on resting state fMRI. J. Neurosci. 32, 10238–10252.
Hinds, O., Polimeni, J.R., Rajendran, N., Balasubramanian, M., Amunts, K., Zilles, K., Schwartz, E.L., Fischl, B., Triantafyllou, C., 2009. Locating the functional and anatomical boundaries of human primary visual cortex. NeuroImage 46, 915–922.
Hirose, S., Watanabe, T., Jimura, K., Katsura, M., Kunimatsu, A., Abe, O., Ohtomo, K., Miyashita, Y., Konishi, S., 2012. Local signal time-series during rest used for areal boundary mapping in individual human brains. PLoS One 7, e36496.
Honey, C.J., Sporns, O., Cammoun, L., Gigandet, X., Thiran, J.P., Meuli, R., Hagmann, P., 2009. Predicting human resting-state functional connectivity from structural connectivity. Proc. Natl. Acad. Sci. U. S. A. 106, 2035–2040.
Hubel, D.H., Wiesel, T.N., 1962. Receptive fields, binocular interaction and functional architecture in the cat's visual cortex. J. Physiol. 160, 106–154.
Jasper, H., Penfield, W., 1954. Epilepsy and the Functional Anatomy of the Human Brain, 2nd ed.
Johansen-Berg, H., Behrens, T.E., Sillery, E., Ciccarelli, O., Thompson, A.J., Smith, S.M., Matthews, P.M., 2005. Functional–anatomical validation and individual variation of diffusion tractography-based segmentation of the human thalamus. Cereb. Cortex 15, 31–39.
Kaas, J.H., Nelson, R.J., Sur, M., Lin, C.S., Merzenich, M.M., 1979. Multiple representations of the body within the primary somatosensory cortex of primates. Science 204, 521–523.
Kahnt, T., Chang, L.J., Park, S.Q., Heinzle, J., Haynes, J.D., 2012. Connectivity-based parcellation of the human orbitofrontal cortex. J. Neurosci. 32, 6240–6250.
Kelly, C., Uddin, L.Q., Shehzad, Z., Margulies, D.S., Castellanos, F.X., Milham, M.P., Petrides, M., 2010. Broca's region: linking human brain functional connectivity data and non-human primate tracing anatomy studies. Eur. J. Neurosci. 32, 383–398.
Kim, J.H., Lee, J.M., Jo, H.J., Kim, S.H., Lee, J.H., Kim, S.T., Seo, S.W., Cox, R.W., Na, D.L., Kim, S.I., Saad, Z.S., 2010. Defining functional SMA and pre-SMA subregions in human MFC using resting state fMRI: functional connectivity-based parcellation method. NeuroImage 49, 2375–2386.
Kim, D.J., Park, B., Park, H.J., 2013. Functional connectivity-based identification of subdivisions of the basal ganglia and thalamus using multilevel independent component analysis of resting state fMRI. Hum. Brain Mapp. 34 (6), 1371–1385 (Jun).
Lancaster, J.L., Glass, T.G., Lankipalli, B.R., Downs, H., Mayberg, H., Fox, P.T., 1995. A modality-independent approach to spatial normalization of tomographic images of the human brain. Hum. Brain Mapp. 3, 209–223.
Leech, R., Braga, R., Sharp, D.J., 2012. Echoes of the brain within the posterior cingulate cortex. J. Neurosci. 32, 215–222.
Margulies, D.S., Vincent, J.L., Kelly, C., Lohmann, G., Uddin, L.Q., Biswal, B.B., Villringer, A., Castellanos, F.X., Milham, M.P., Petrides, M., 2009. Precuneus shares intrinsic functional architecture in humans and monkeys. Proc. Natl. Acad. Sci. U. S. A. 106, 20069–20074.
Mars, R.B., Sallet, J., Schuffelgen, U., Jbabdi, S., Toni, I., Rushworth, M.F., 2012. Connectivity-based subdivisions of the human right "temporoparietal junction area": evidence for different areas participating in different cortical networks. Cereb. Cortex 22, 1894–1903.
Marshall, W.H., Woolsey, C.N., Bard, P., 1937. Cortical representation of tactile sensibility as indicated by cortical potentials. Science 85, 388–390.
Miezin, F.M., Maccotta, L., Ollinger, J.M., Petersen, S.E., Buckner, R.L., 2000. Characterizing the hemodynamic response: effects of presentation rate, sampling procedure, and the possibility of ordering brain activity based on relative timing. NeuroImage 11, 735–759.
Mugler III, J.P., Brookeman, J.R., 1990. Three-dimensional magnetization-prepared rapid gradient-echo imaging (3D MP RAGE). Magn. Reson. Med. 15, 152–157.
Mumford, J.A., Horvath, S., Oldham, M.C., Langfelder, P., Geschwind, D.H., Poldrack, R.A., 2010. Detecting network modules in fMRI time series: a weighted network analysis approach. NeuroImage 52, 1465–1476.
Nelson, S.M., Cohen, A.L., Power, J.D., Wig, G.S., Miezin, F.M., Wheeler, M.E., Velanova, K., Donaldson, D.I., Phillips, J.S., Schlaggar, B.L., Petesen, S.E., 2010a. A parcellation scheme for human left lateral parietal cortex. Neuron 67, 156–170.
Nelson, S.M., Dosenbach, N.U., Cohen, A.L., Wheeler, M.E., Schlaggar, B.L., Petersen, S.E., 2010b. Role of the anterior insula in task-level control and focal attention. Brain Struct. Funct. 214, 669–680.
Ojemann, J.G., Akbudak, E., Snyder, A.Z., McKinstry, R.C., Raichle, M.E., Conturo, T.E., 1997. Anatomic localization and quantitative analysis of gradient refocused echo-planar fMRI susceptibility artifacts. NeuroImage 6, 156–167.
Ongur, D., Ferry, A.T., Price, J.L., 2003. Architectonic subdivision of the human orbital and medial prefrontal cortex. J. Comp. Neurol. 460, 425–449.
Petersen, S.E., Fox, P.T., Posner, M.I., Mintun, M., Raichle, M.E., 1988. Positron emission tomographic studies of the cortical anatomy of single-word processing. Nature 331, 585–589.
Power, J.D., Cohen, A.L., Nelson, S.M., Wig, G.S., Barnes, K.A., Church, J.A., Vogel, A.C., Laumann, T.O., Miezin, F.M., Schlaggar, B.L., Petersen, S.E., 2011. Functional network organization of the human brain. Neuron 72, 665–678.
Power, J.D., Barnes, K.A., Snyder, A.Z., Schlaggar, B.L., Petersen, S.E., 2012. Spurious but systematic correlations in functional connectivity MRI networks arise from subject motion. NeuroImage 59, 2142–2154.
Ryali, S., Chen, T., Supekar, K., Menon, V., 2013. A parcellation scheme based on von Mises–Fisher distributions and Markov random fields for segmenting brain regions using resting-state fMRI. NeuroImage 65, 83–96.
Sabuncu, M.R., Singer, B.D., Conroy, B., Bryan, R.E., Ramadge, P.J., Haxby, J.V., 2010. Function-based intersubject alignment of human cortical anatomy. Cereb. Cortex 20, 130–140.
Satterthwaite, T.D., Wolf, D.H., Loughead, J., Ruparel, K., Elliott, M.A., Hakonarson, H., Gur, R.C., Gur, R.E., 2012. Impact of in-scanner head motion on multiple measures of functional connectivity: relevance for studies of neurodevelopment in youth. NeuroImage 60, 623–632.
Schleicher, A., Zilles, K., 1990. A quantitative approach to cytoarchitectonics: analysis of structural inhomogeneities in nervous tissue using an image analyser. J. Microsc. 157, 367–381.
Scholvinck, M.L., Maier, A., Ye, F.Q., Duyn, J.H., Leopold, D.A., 2010. Neural basis of global resting-state fMRI activity. Proc. Natl. Acad. Sci. U. S. A. 107, 10238–10243.
Schormann, T., Zilles, K., 1998. Three-dimensional linear and nonlinear transformations: an integration of light microscopical and MRI data. Hum. Brain Mapp. 6, 339–347.
Ségonne, F., Dale, A.M., Busa, E., Glessner, M., Salat, D., Hahn, H.K., Fischl, B., 2004. A hybrid approach to the skull stripping problem in MRI. NeuroImage 22, 1060–1075.
Ségonne, F., Grimson, E., Fischl, B., 2005. A genetic algorithm for the topology correction of cortical surfaces. Inf. Process. Med. Imaging 19, 393–405.
Sejnowski, T.J., Churchland, P.S., 1989. Brain and cognition. In: Posner, M. (Ed.), Foundations of Cognitive Science. MIT Press, Cambridge, p. 888.
Sereno, M.I., Dale, A.M., Reppas, J.B., Kwong, K.K., Belliveau, J.W., Brady, T.J., Rosen, B.R., Tootell, R.B., 1995. Borders of multiple visual areas in humans revealed by functional magnetic resonance imaging. Science 268, 889–893.
Smith, S.M., Fox, P.T., Miller, K.L., Glahn, D.C., Fox, P.M., Mackay, C.E., Filippini, N., Watkins, K.E., Toro, R., Laird, A.R., Beckmann, C.F., 2009. Correspondence of the brain's functional architecture during activation and rest. Proc. Natl. Acad. Sci. U. S. A. 106, 13040–13045.
Smith, S.M., Miller, K.L., Moeller, S., Xu, J., Auerbach, E.J., Woolrich, M.W., Beckmann, C.F., Jenkinson, M., Andersson, J., Glasser, M.F., Van Essen, D.C., Feinberg, D.A., Yacoub, E.S., Ugurbil, K., 2012. Temporally-independent functional modes of spontaneous brain activity. Proc. Natl. Acad. Sci. U. S. A. 109, 3131–3136.
Snyder, A.Z., 1996. Difference image vs. ratio image error function forms in PET–PET realignment. In: Myer, R., Cunningham, V.J., Bailey, D.L., Jones, T. (Eds.), Quantification of Brain Function using PET. Academic Press, San Diego, CA, pp. 131–137.
Talairach, J., Tournoux, P., 1988. Co-planar Stereotaxic Atlas of the Human Brain. Thieme Medical Publishers, Inc., New York.
Toga, A.W., Thompson, P.M., Mori, S., Amunts, K., Zilles, K., 2006. Towards multimodal atlases of the human brain. Nat. Rev. Neurosci. 7, 952–966.
Uddin, L.Q., Supekar, K., Amin, H., Rykhlevskaia, E., Nguyen, D.A., Greicius, M.D., Menon, V., 2010. Dissociable connectivity within human angular gyrus and intraparietal sulcus: evidence from functional and structural connectivity. Cereb. Cortex 20, 2636–2646.
Van Dijk, K.R., Sabuncu, M.R., Buckner, R.L., 2012. The influence of head motion on intrinsic functional connectivity MRI. NeuroImage 59, 431–438.
Van Essen, D.C., 2005. A Population-Average, Landmark- and Surface-based (PALS) atlas of human cerebral cortex. NeuroImage 28, 635–662.
Van Essen, D.C., Maunsell, J.H., Bixby, J.L., 1981. The middle temporal visual area in the macaque: myeloarchitecture, connections, functional properties and topographic organization. J. Comp. Neurol. 199, 293–326.
Van Essen, D.C., Drury, H.A., Dickson, J., Harwell, J., Hanlon, D., Anderson, C.H., 2001. An integrated software suite for surface-based analyses of cerebral cortex. J. Am. Med. Inform. Assoc. 8, 443–459.
Van Essen, D.C., Glasser, M.F., Dierker, D.L., Harwell, J., Coalson, T., 2012. Parcellations and hemispheric asymmetries of human cerebral cortex analyzed on surface-based atlases. Cereb. Cortex 22 (10), 2241–2262 (Oct).
Van Essen, D.C., Ugurbil, K., Auerbach, E., Barch, D., Behrens, T.E., Bucholz, R., Chang, A., Chen, L., Corbetta, M., Curtiss, S.W., Della Penna, S., Feinberg, D., Glasser, M.F., Harel, N., Heath, A.C., Larson-Prior, L., Marcus, D., Michalareas, G., Moeller, S., Oostenveld, R., Petersen, S.E., Prior, F., Schlaggar, B.L., Smith, S.M., Snyder, A.Z., Xu, J., Yacoub, E., 2012. The Human Connectome Project: a data acquisition perspective. NeuroImage 62, 2222–2231.
Vincent, J.L., Patel, G.H., Fox, M.D., Snyder, A.Z., Baker, J.T., Van Essen, D.C., Zempel, J.M., Snyder, L.H., Corbetta, M., Raichle, M.E., 2007. Intrinsic functional architecture in the anesthetized monkey brain. Nature 447, 46–47.
Vogt, O., Vogt, C., 1919. Allgemeine Ergebnisse unserer Hirnforschung. J. Psychol. Neurol. 25, 273–462.
Wasserman, S., Faust, K., 1994. Social Network Analysis: Methods and Applications. Cambridge University Press, Cambridge.
Wig, G.S., Schlaggar, B.L., Petersen, S.E., 2011. Concepts and principles in the analysis of brain networks. Ann. N. Y. Acad. Sci. 1224, 126–146.
Wig, G.S., Laumann, T.O., Cohen, A.L., Power, J.D., Nelson, S.M., Glasser, M.F., Miezin, F.M., Snyder, A.Z., Schlaggar, B.L., Petersen, S.E., 2013. Parcellating an individual subject's cortical and subcortical brain structures using snowball sampling of resting-state correlations. Cereb. Cortex. http://dx.doi.org/10.1093/cercor/bht056 (first published online March 8, 2013).
Yeo, B.T., Krienen, F.M., Sepulcre, J., Sabuncu, M.R., Lashkari, D., Hollinshead, M., Roffman, J.L., Smoller, J.W., Zollei, L., Polimeni, J.R., Fischl, B., Liu, H., Buckner, R.L., 2011. The organization of the human cerebral cortex estimated by intrinsic functional connectivity. J. Neurophysiol. 106, 1125–1165.
Zar, J., 1996. Biostatistical Analysis. Prentice Hall, Upper Saddle River, NJ.
Zhang, D., Snyder, A.Z., Fox, M.D., Sansbury, M.W., Shimony, J.S., Raichle, M.E., 2008. Intrinsic functional relations between human cerebral cortex and thalamus. J. Neurophysiol. 100, 1740–1748.